THE ASTROPHYSICAL JOURNAL SUPPLEMENT SERIES, 36:285–304, 1978 February

THE *p*-PROCESS IN SUPERNOVAE

S. E. WOOSLEY
Lick Observatory, Board of Studies in Astronomy and Astrophysics, University of California, Santa Cruz
AND
W. M. HOWARD
University of California, Lawrence Livermore Laboratory, Livermore, California
Received 1976 December 27; accepted 1977 August 12

ABSTRACT

The nucleosynthetic origin of the rare proton-rich isotopes, usually called "*p*-process" isotopes, is examined. A particularly interesting context for this synthesis is found to be explosive events characterized by peak temperatures in the range 2.0 to 3.0 × 10^9 K. At these temperatures a series of photodisintegration reactions operating upon a distribution of *r*- and *s*-process seeds produces an abundance pattern that displays striking similarities to that of the *p*-process nuclei in the solar system. The large proton densities usually required for such synthesis are not needed. Requisite conditions for this model are expected to occur naturally in those zones of supernovae that have experienced helium and perhaps carbon burning prior to explosion. Implications for supernova structure, presupernova evolution, and cosmochronology are discussed and a critical discussion of other current *p*-process models is presented.

Subject headings: nucleosynthesis — stars: abundances — stars: supernovae

I. INTRODUCTION

The "*p*-process" isotopes or "*p*-nuclei" are those stable nuclear isotopes with mass number $A \geq 74$ that lie on the proton-rich side of the valley of beta-stability and are bypassed by the neutron capture chains (*r*- and *s*-processes) that are responsible for producing the bulk of the heavy elements. As a group they are the rarest of all stable nuclei. In fact, no single element has as a dominant constituent a *p*-process isotope. Consequently all knowledge of abundance systematics for these species is based entirely upon solar-system measurements (Cameron 1973). Typically, *r*- and *s*-process nuclei in the solar system have abundances that are 10^2 to 10^3 times larger than adjacent *p*-nuclei, and it is generally accepted that these much more abundant species somehow serve as progenitors of the *p*-nuclei through an as yet poorly understood mechanism that probably occurs in supernovae.

Those isotopes traditionally attributed to the *p*-process are listed in Table 1 along with their abundances by mass fraction in the solar system and designations as to whether they are even, odd, or odd-particle nuclei. Possible *s*-process contributions are also noted. In all that follows, we shall employ the term "*p*-nuclei" to refer to this set of species (regardless of their synthesis mechanism). The "*p*" may be thought of as designating the fact that these nuclei are proton-rich relative to other stable isotopes of the same element.

It is readily apparent that most of these nuclei have even numbers of neutrons and protons. Those few species with odd neutron and proton number (^{138}La and ^{180}Ta) are of considerably smaller abundance, and the only *p*-nuclei with odd mass numbers (^{113}In and ^{115}Sn) may be made by the *s*-process. Thus it appears that *all* nuclei produced in sizable amounts by the *p*-process are even nuclei, a fact which presumably reflects the decreased stability of a nucleus with an unpaired proton or neutron in the environment where the synthesis occurs. This sensitivity to nuclear binding energy is further reflected in the existence of relative abundance peaks at ^{92}Mo, ^{112}Sn, ^{144}Sm, and ^{164}Er. The nuclei ^{92}Mo and ^{144}Sm have closed neutron shells, and ^{112}Sn has a closed proton shell.

The astrophysical circumstances under which the *p*-nuclei were assembled have been a subject of controversy for almost 20 years. Cameron (1957) and Burbidge *et al.* (1957, henceforth B^{2}FH) proposed that these nuclei are produced in the hydrogen-rich layers of type II supernovae. There a combination of (p, γ) and (γ, n) reactions operating on a preexisting set of *r*- and *s*-process seeds can produce a set of nuclei that are shielded from production by neutron capture. Because of the dominant role played by proton reactions, B^{2}FH named these the "*p*-process nuclei" and suggested that for temperatures on the order of 2.5 billion degrees, and proton densities of roughly 100 g cm^{-3}, such conversion could take place on a local hydrodynamic time scale (10–100 s). Since 1957 many mechanisms have been studied for the conversion of heavy elements into *p*-nuclei, including spallation reactions (Frank-Kamenetskii 1961; Audouze 1970; Hainebach, Schramm, and Blake 1976); positron capture and photo-beta processes (Cameron 1959; Reeves and Stewart 1965; Arnould and Brihaye 1969; Joukoff 1969; Agnese, La Camera,

TABLE 1

THE p-PROCESS NUCLEI (Abundances from Cameron 1973)

Nucleus	Particle Designation	Solar System Mass Fraction
^{74}Se.........	Even	1.04 (−9)
^{78}Kr.........	Even	3.13 (−10)
^{84}Sr..........	Even	3.06 (−10)
^{92}Mo........	Even	1.41 (−9)
^{94}Mo*.......	Even	8.22 (−10)
^{96}Ru........	Even	2.43 (−10)
^{98}Ru.........	Even	8.40 (−11)
^{102}Pd.........	Even	3.08 (−11)
^{106}Cd.........	Even	4.61 (−11)
^{108}Cd†........	Even	3.39 (−11)
^{113}In‡........	Odd particle	2.18 (−11)
^{112}Sn.........	Even	9.36 (−11)
^{114}Sn‡........	Even	6.55 (−11)
^{115}Sn‡........	Odd particle	3.50 (−11)
^{120}Te.........	Even	1.65 (−11)
^{124}Xe.........	Even	2.03 (−11)
^{126}Xe.........	Even	1.88 (−11)
^{130}Ba.........	Even	1.52 (−11)
^{132}Ba.........	Even	1.49 (−11)
^{136}Ce.........	Even	7.49 (−12)
^{138}Ce.........	Even	9.83 (−12)
^{138}La.........	Odd	1.37 (−12)
^{144}Sm.........	Even	2.43 (−11)
^{152}Gd§........	Even	2.18 (−12)
^{156}Dy.........	Even	7.12 (−13)
^{158}Dy.........	Even	1.24 (−12)
^{162}Er.........	Even	1.20 (−12)
^{164}Er.........	Even	1.39 (−11)
^{168}Yb.........	Even	1.18 (−12)
^{174}Hf.........	Even	1.60 (−12)
^{180}Ta.........	Odd	1.12 (−14)
^{180}W.........	Even	9.39 (−13)
^{184}Os.........	Even	6.00 (−13)
^{190}Pt.........	Even	8.17 (−13)
^{196}Hg.........	Even	2.76 (−12)

* Bypassed by s-process if time scale for neutron capture on ^{93}Zr is much less than 1.5×10^6 yr.

† Bypassed by s-process if time scale for neutron capture on ^{107}Pd is much less than 7×10^6 yr.

‡ Some s-process contribution if a branch proceeds through the isomeric state of ^{113}Cd. Also ^{115}Sn is formed by 5% of neutron captures on ^{114}Cd that leave ^{115}Cd in its ground state.

§ On s-branch since a significant fraction of ^{151}Sm will beta-decay.

and Wataghin 1969); and the thermonuclear reactions (p, γ), (p, n), (γ, n), (γ, p), and (γ, α) (Ito 1961; Frank-Kamenetskii 1961; Malkiel 1963; Amiet and Zeh 1967, 1968; Macklin 1970; Truran and Cameron 1972; Truran 1973; Audouze and Truran 1975, henceforth AT; Arnould 1976). For realistic astrophysical environments spallation reactions prove ineffective in accounting for all but the rarest of the p-nuclei. Weak interactions induced by the high-temperature photon and positron baths also appear to be very unlikely candidates for p-nucleosynthesis. Such reactions would proceed at rates that are extremely sensitive functions of individual nuclear excited-state configurations. One would expect the product nucleosynthesis to vary much more sharply from nucleus to nucleus than is reflected in Table 1. Another severe objection to this type of synthesis is that at the high temperatures required to make photon-induced weak interactions occur at reasonable rates (cf. Reeves and Stewart 1965), photodisintegration reactions, notably (γ, n), would destroy the seed abundance in a time scale that is, in all but a few cases, shorter than the time required for significant weak interaction. Finally, one must confront the problem that such processes leave the product nuclei still tightly bound within a star. Any explosion significantly powerful to eject them would probably modify the composition. This same objection also applies to a recent treatment by Arnould (1976) of the p-process during hydrostatic oxygen burning. While his work surpasses in many ways all previous attempts to make the p-nuclei during stable stellar evolution, it does not appear likely that the products of this evolution can be ejected into the interstellar medium without significant reprocessing.

For these reasons models based upon *explosive* nucleosyntheses in supernovae appear more attractive candidates for the production of the p-nuclei. Thus far most studies of this sort have followed the lead of B^{2}FH and Cameron (1957) in limiting themselves to hydrogen-rich regions where (p, γ) reactions play an important role. In particular, the success of AT is quite impressive in reproducing the qualitative features of the abundance pattern of p-nuclei. However, it is our contention that these models, while mathematically successful, may require physical conditions that cannot easily be realized in nature. Furthermore, several of the assumptions inherent in these models may be unjustified. This is a topic we shall discuss in greater detail in the next section.

In § III an alternative mechanism is presented for the synthesis of p-nuclei which is more properly called the "γ-process." It is shown that a distribution of heavy elements subjected to a hot *photon* bath having radiation temperatures in the range $2.1 \leq T_9 \leq 3.2$ (where T_9 is temperature in billions of degrees) will be transformed on a time scale of roughly 1 s into a distribution of elements that resembles closely the solar abundance pattern of p-nuclei. The transformation occurs via a series of (γ, n), (γ, p), and (γ, α) reactions that act to strip down or "photodisintegrate" the seed nuclei into lighter products. Amiet and Zeh (1967, 1968) described a similar mechanism for producing the p-nuclei, although they gave very little quantitative detail. Unlike other scenarios for the p-process that utilize protons, the γ-process does not form a product nucleus of nuclear charge Z_p solely from seed having $Z \leq Z_p$. In our calculations the seed abundance of ^{208}Pb, for example, can and does affect the production of lighter species like ^{144}Sm. Our calculations also differ from those of AT, B^{2}HF, and others in that (p, γ) and (p, n) reactions play no role. Thus the large proton densities usually required for the p-process do not appear. In fact, we view the requisite conditions for synthesizing the p-nuclei as occurring most naturally in those zones of a type II supernova that have exhausted hydrogen, helium, and probably carbon. In their simplest form our results are independent of the exact composition and density of the zones treated. Only the abundances of seed nuclei and the distribution of *photon* temperatures matter.

Before discussing in greater detail the methodology and results of these calculations, however, it is useful to first consider the status of other current models for p-nucleosynthesis in supernovae. In particular, what are the weaknesses in the calculations of B^{2}FH, AT, and others that lead us to search for alternative sites and methods for producing these nuclei?

II. PROBLEMS WITH CURRENT EXPLOSIVE MODELS

Models of the explosive p-process in hydrogen zones that exist in the literature all share the following set of "canonical" assumptions (cf. B^{2}FH, AT):

1. The required synthesis occurs in hydrogen zones of a supernova that during their explosive ejection attain temperatures in excess of 2×10^9 K. At this temperature a balance is attained whereby photoneutron reactions occurring on heavy seed nuclei and proton capture on lighter seed nuclei proceed at comparable rates, making possible the synthesis of all p-nuclei at a nearly unique value of temperature. The time scale for the expansion is assumed to be equal to the local hydrodynamic time scale, $\tau_{\mathrm{HD}} = 446/(\rho_b)^{1/2}$ s for ρ_b in g cm^{-3}. Values of ρ_b in the range 10^2 to 10^4 g cm^{-3} are usually employed.
2. Weak interactions are negligible during the synthesis.
3. The distribution of seed nuclei is like the solar abundance distribution of heavy elements.

We find serious flaws in each of these assumptions.

a) *Thermodynamic Conditions*

Can temperatures as high as 2×10^9 K be achieved for times as long as 10 seconds in the *hydrogen*-rich zones of any common astrophysical event? It does not appear likely. Under such conditions the energy contained in the radiation field per gram of baryon mass would be

$$E_\gamma = aT^4/\rho_b = 1.21 \times 10^{23}/\rho_b \text{ ergs g}^{-1}, \qquad (1)$$

where ρ_b is the matter density in g cm^{-3} and a value of 2×10^9 K has been inserted for T. Exclusive of hydrogen burning itself, nuclear reactions can generate only about 10^{18} ergs g^{-1}. Observed supernova expansion velocities imply an energy input of similar magnitude. Unless the energy output of a supernova can somehow be concentrated in those zones responsible for the p-process, a lower limit to the baryon mass density must be $\rho_b \gtrsim 10^5$ g cm^{-3}. Another way of seeing this same result is to consider the energy requirements for heating roughly 0.01 $M_\odot$ of baryons to 2×10^9 K in equilibrium with a radiation field of the same temperature. The value 0.01 $M_\odot$ is the amount of material per supernova that AT predict must experience p-processing to account for the present abundances *even if the seed abundances have been enhanced by a factor of 100!* If no enhancement has occurred, a correspondingly larger mass must be specified. This mass and an average density imply a volume of radiation energy that must be deposited within that 0.01 $M_\odot$ of baryons. That energy is

$$E_\gamma = \frac{2.4 \times 10^{54}}{\rho_b} \frac{M}{0.01\, M_\odot} \text{ ergs}. \qquad (2)$$

If no seed enrichment has occurred a larger value is required. A typical supernova explosion generates approximately 10^{52} ergs, most of which goes into neutrino emission and kinetic energy of expansion (Schramm and Arnett 1975). We conclude $\rho_b \gtrsim 10^3$ g cm^{-3} is required in those zones specified by AT as the site of p-process synthesis even if seed enrichment has occurred and a large fraction of the total energy output of a supernova can somehow be concentrated in those zones. Since realistically only a small fraction of the total energy of a supernova can be deposited in 0.01 $M_\odot$, the density required is actually much larger.

Where in the Galaxy do hydrogen zones of such density exist? Certainly they do not exist in the hydrogen envelopes of ordinary stars. Typical densities at the base of the *helium* burning shells of highly evolved stars are on the order of 10^3 g cm^{-3} (Lamb, Iben, and Howard 1976). Densities in the overlying hydrogen burning shells would be a great deal smaller. The occurrence of the requisite condition in supernovae therefore seems unlikely. Large proton densities *can* be found on the surface of an accreting white dwarf, and during a *nova* outburst this hydrogen may, in some extreme cases, be heated to 2×10^9 K (Starrfield, Truran, and Sparks 1975). However, the time scale for such an extreme temperature is short ($\lesssim 0.1$ s), and the amount of material processed is small.

b) *Role of Weak Interactions*

In their early calculations of p-process synthesis B^{2}FH chose to ignore the weak interactions $(e^+\nu)$ and (e^-, ν) that would occur during the conversion of r- and s-seed into p-nuclei and their progenitors. This neglect was based upon a certain set of assumptions: (i) the time scale for the p-process is 10 to 100 seconds, (ii) proton capture ceases when the proton separation energy of any product nucleus becomes less than 4.3 MeV, and (iii) all weak interactions have matrix elements characteristic of forbidden decays. The result of assumptions (ii) and (iii) was to yield a minimum expected positron decay time of about 10^3 s. This was long compared to assumption (i), and hence weak interactions were negligible.

Following these preliminary calculations, all subsequent works have also chosen to ignore weak interactions, even though the circumstances nowadays dictated for the synthesis differ in key ways from the earlier work. The limiting proton separation energy where (p, γ) addition will stop, for example, was computed by B^{2}FH assuming a proton-link equilibrium calculated at $T_9 = 2.5$ and $\rho_b = 10^2$ g cm^{-3}. Use of the more modern conditions employed by AT, namely $T_9 = 2.0$ and $\rho_b = 10^4$ g cm^{-3}, in equation (26) of B^{2}FH now yields $S_p = 2.6$ MeV instead of the value 4.3 that B^{2}FH employed. Furthermore, since modern calculations are performed within an explosive context where the temperature decreases with time rather than at constant temperature, one can expect still further penetration as the temperature falls to lower values. Such behavior is expected because the reaction rates for (γ, p) reactions are more temperature-sensitive than for (p, γ) reactions. Species near the proton drip line will be formed.

The lifetimes of such species are difficult to estimate but it seems doubtful that their decay will be limited to forbidden transitions. Takahashi, Yamada, and Kondoh (1973), using the gross theory of beta decay, calculate half-lives as short as 1 s for nuclei with proton separation energies of 2.6 MeV near the proton drip line in the mass region of the *p*-nuclei. Since expansion time scales of 5 to 50 seconds are typical in these calculations, weak interactions must be considered at least for the lighter nuclei. The propagation of abundant seed material upward from ^{56}Fe into the lighter *p*-nuclei is a distinct possibility.

c) Distribution of Seed Nuclei

How realistic is it to adopt a solar distribution of heavy elements as seeds for the *p*-process? If no *s*-processing has occurred during the preexplosive evolution, it may be an excellent approximation, but, as mentioned before (§ II*a*), producing the bulk of *p*-nuclei in nonenriched zones places severe energy requirements on the explosion. Therefore, the more realistic approach typified by AT demands large enhancements of heavy elements, presumably by prior *s*-processing in or near the zones considered. One obvious implication is that only those seed nuclei which are due to the *s*-process should be so enhanced, i.e., not the *r*-process seed (Arnould 1976). This in itself probably changes results of the *p*-process very little since the *r*-process nuclei are not especially important seeds. What can alter the situation substantially, however, and what is very difficult to estimate, is the distribution of *elements* in the interior of stars that have done *s*-processing. This set of abundances is a complicated function of the mass, composition, and evolutionary state of the star when it explodes. There is no *a priori* reason to believe the distribution should resemble solar *s*-process abundances.

III. THE γ-PROCESS

We now present our theory of the *p*-process which for reasons that will shortly become obvious is more properly called the "γ-process." We will find that the objections raised in the previous section with regard to energetics and weak interactions can be circumvented, but the nature of the seed distribution and the sensitivity of the results to unknown explosion parameters remain severe problems.

a) The Photodisintegration of Heavy Elements

Consider a heavy element in the presence of a photon bath sufficiently intense to induce nuclear reactions. For stable elements that are produced by the *r*- and *s*-processes the nuclear systematics are such that the dominant photon-induced reaction will be (γ, n). The rate of neutron ejection is given by

$$\lambda_{\gamma n} = C T_9^{3/2} \exp\left[-11.605 S_n(\mathrm{MeV})/T_9\right] \mathrm{s}^{-1}, \quad (3)$$

where C is a slowly varying function of temperature and nuclear properties and S_n is the neutron separation energy of the species under consideration (Fowler, Caughlan, and Zimmerman 1967). With each neutron ejected S_n becomes, on the average, larger, and the rate of the photo-neutron reaction slower. At the same time the separation energy for a proton or α-particle is decreasing and the rate for photodisintegration accompanied by charged-particle emission is increasing. For example, the rate of the (γ, α) reaction on a nucleus with Z protons is roughly given by

$$\lambda_{\gamma\alpha} = D T_9^{5/6} \exp\left[-\tau_\alpha/T_9^{1/3} - 11.605 S_\alpha(\mathrm{MeV})/T_9\right] \mathrm{s}^{-1},$$

$$\tau_\alpha = 4.2487(4Z^2\bar{A})^{1/3} \approx 10.7(Z-2)^{2/3}, \quad (4)$$

where $\bar{A}$ is the reduced mass, roughly equal to 4, S_α is the α-particle separation energy, and D is again a relatively slowly varying function of temperature and nuclear properties. A similar expression could be written for $\lambda_{\gamma p}$. As neutrons continue to be ejected, a point is eventually reached where $\lambda_{\gamma p} + \lambda_{\gamma\alpha} > \lambda_{\gamma n}$, and it becomes energetically more feasible for the nucleus to eject a charged particle than a neutron, even though the former experiences a sizable Coulomb hindrance. That point is defined for heavy nuclei of even charge and mass (for which it usually turns out that $\lambda_{\gamma p} \ll \lambda_{\gamma\alpha}$) by the expression

$$S_n - S_\alpha \gtrsim 0.0862\left[\tau_\alpha T_9^{2/3} - T_9 \ln\left(D/C T_9^{2/3}\right)\right] \mathrm{MeV}. \quad (5)$$

Rough estimates for the constants C and D can be obtained from formulae given by Woosley *et al.* (1975). Evaluation of equation (5) at $T_9 = 3$, for example, yields critical values of $S_n - S_\alpha$ ranging from roughly 7 MeV for $Z = 40$ to about 13 MeV for $Z = 82$. Higher values of temperature result in somewhat larger values for $S_n - S_\alpha$ and therefore indicate nuclei that are increasingly proton-rich.

A more accurate calculation of the branching point is possible using the reaction rates computed in Appendix A to numerically locate those points where $\lambda_{\gamma p} + \lambda_{\gamma\alpha} > \lambda_{\gamma n}$ (see Table 7). The results of such a numerical comparison are listed in Table 2 for a typical value of temperature ($T_9 = 2.5$) along with a designation of the favored type of charged-particle emission. For heavy even nuclei the particle ejected is almost invariably an alpha, while for odd nuclei and light nuclei proton ejection also plays a role. Even though we have listed only the branching points where charged-particle emission clearly dominates, it should be apparent that other neighboring nuclei with even

TABLE 2

BRANCHING POINTS FOR HEAVY ELEMENTS UNDERGOING PHOTODISINTEGRATION AT $T_9 = 2.5$

Element	x	$A[\lambda_{\gamma x} > \lambda_{\gamma n}]$	Element	x	$A[\lambda_{\gamma x} > \lambda_{\gamma n}]$	Element	x	$A[\lambda_{\gamma x} > \lambda_{\gamma n}]$
Bi	p	201	Dy	α	154	Sn	p, α	110
Pb	α	194	Tb	α	151	In	p	111
Tl	p	195	Gd	α	150	Cd	α	106
Hg	α	188	Eu	α	147	Ag	p	105
Au	p, α	187	Sm	p	142	Pd	α	100
Pt	α	184	Pm	p	143	Rh	p	101
Ir	α, p	183	Nd	p, α	138	Ru	α	96
Os	α	180	Pr	p	139	Tc	p	95
Re	p, α	177	Ce	α	134	Mo	p	92
W	α	174	La	p	133	Nb	p	91
Ta	p	171	Ba	p, α	126	Zr	p	90
Hf	α	168	Cs	p	129	Y	p	89
Lu	p	167	Xe	α	122	Sr	p	84
Yb	α	164	I	p	123	Rb	p	85
Tm	p	161	Te	α	120	Kr	p	78
Er	α	158	Sb	p	119	Br	p	79
Ho	p	157				Se	α	74

numbers of neutrons may also be sites of significant branching. Nuclei with odd neutron numbers that have masses greater than the numbers given in Table 2 are not branching points because the rate of (γ, n) reactions on such nuclei is always large and dominates in their destruction.

One immediate consequence of Table 2 is that weak interactions will be completely negligible for the γ-process so long as one considers (i) temperatures in the range of 2–3 billion degrees or less and (ii) time scales less than about 100 seconds. The limiting time-scale value comes from an examination of the laboratory half-lives of species in Table 2.

Once the photodisintegration flow for a given element reaches the critical point given in equation (5), further photon interaction will lead to a change in the nuclear charge of the element, a decrease by 2 in the case of alpha emission. The product nucleus thus formed may once again find it energetically feasible to eject neutrons or it too may eject a charged particle. If it ejects neutrons another waiting point is eventually reached where charged-particle emission occurs and the process continues. Ultimately the original heavy nucleus is photodissociated into a mixture of iron-group nuclei and free neutrons, protons, and alphas. A state of nuclear statistical equilibrium is attained.

The extreme case of total photodissociation is not of interest here nor are the free particles that are ejected by this γ-process. They will presumedly just form a negligible perturbation on the more dominant particle-producing reactions in the site where the process occurs (see § IV). What is of considerable interest, however, is the nucleosynthesis that occurs for values of temperature and time scale that are sufficient to induce some nuclear transformation yet not so intense as to totally reduce all heavy elements to iron. Instead of a single nucleus one may envision a distribution of seed nuclei extending up to lead, all subject to the same intense radiation bath. Then the flow of material down from lead toward iron forms a stream with many tributaries, each stretching back to some particular seed nucleus. Here and there are various points where the flow is impeded because some nucleus has an unusually long lifetime. For each element of nuclear charge Z the longest photodisintegration lifetimes on the flow path tend to occur near the branch points given in Table 2. Material will accumulate at or near these waiting points, especially for nuclei with a closed neutron or proton shell. Very little material will accumulate at odd and odd-particle nuclei.

This behavior is qualitatively illustrated in Figure 1, which shows for a representative temperature ($T_9 = 2.5$) the dominant photodisintegration flows for the heaviest nuclei considered. The very interesting aspect of such a scenario is that for a reasonable range of temperatures, namely $2 \lesssim T_9 \lesssim 3$, waiting points seem to correspond either to the p-nuclei or to nuclei that would decay to p-nuclei by positron emission after ejection. This range of temperatures is also of special interest because at such temperatures heavy nuclei are partially but not totally photodisintegrated. For $Z \leq 66$ the p-nuclei themselves are waiting points. For higher Z the correspondence is to proton-rich progenitors having the same atomic weight as the p-nuclei but a nuclear charge larger by 2. For example, ^{196}Hg is produced as ^{196}Pb, ^{190}Hg as ^{190}Pt, and so on down to the element erbium. Such a correspondence suggests that the nuclei attributed to the p-process may not have originated in a proton-rich environment at all but instead in a photon-dominated process.

If this conjecture is correct, one might expect a correlation between the observed solar abundances of the p-nuclei and their photodisintegration rates. That such a correlation does indeed exist was pointed out by Macklin (1970). However, Macklin suggested that this correlation had only to do with the lifetime against (γ, n) reactions (and hence neutron separation energy) and ignored the role of (γ, p) and (γ, α). He also neglected the possibility that the abundances of several p-nuclei might reflect the nuclear properties of

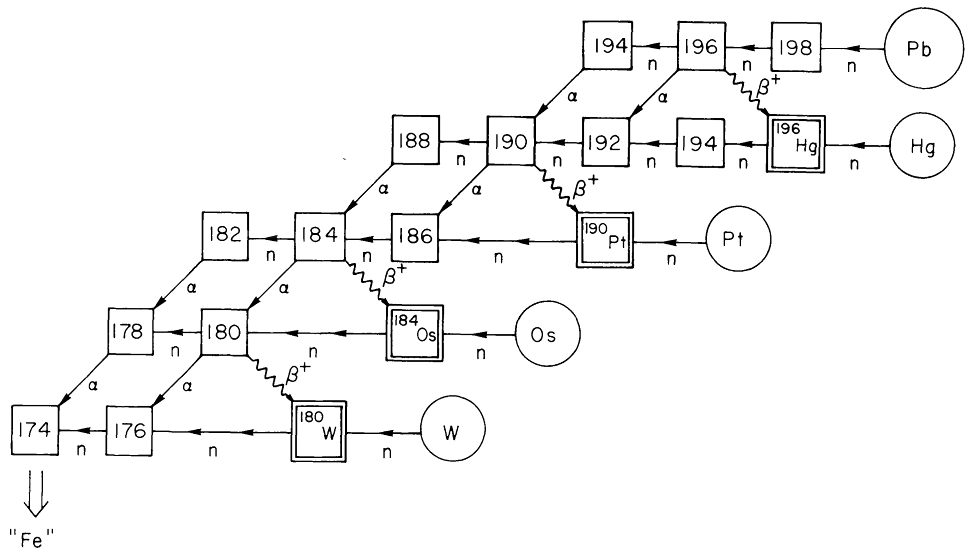

FIG. 1.—Photodisintegration flows in the vicinity of the heavy p-nuclei (*double squares*). The circles labeled with elemental symbols represent all the stable isotopes of the given element. Arrows labeled with "n" or "α" represent photo-neutron and photo-alpha flows, respectively. In this mass region and at this temperature the p-nuclei are primarily produced as proton-rich progenitors which decay by positron emission (arrows labeled β^+) after the explosion.

progenitors rather than those of themselves. Nevertheless, Macklin's plots of abundance and neutron separation energy show striking correlation.

A more proper approach would be to compare the solar abundance pattern to a plot of *total* photodisintegration rate $\Lambda \equiv \lambda_{\gamma n} + \lambda_{\gamma p} + \lambda_{\gamma\alpha}$ for the p-nuclei and, where appropriate, their proton-rich progenitors. We have prepared such a plot using the photodisintegration rates given in Table 7 for a temperature $T_9 = 3$ and the solar abundances as given by Cameron (1973). Only those nuclei directly attributable to the p-process are included in this plot; i.e., nuclei that have footnotes in Table 1 are not included. The results are shown in Figure 2. One is

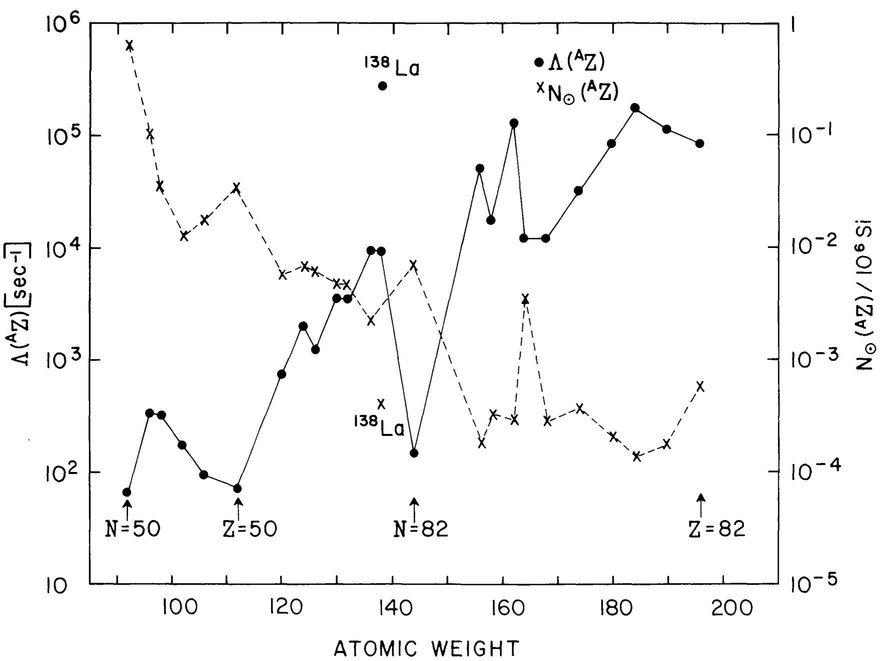

FIG. 2.—Total photodisintegration rates Λ for the p-nuclei and their proton-rich progenitors at $T_9 = 3.0$ as a function of their mass number. Also shown is a plot of their solar abundance by number relative to 10^6 silicon atoms. The arrows indicate p-nuclei with closed neutron or proton shells. The abundance of the p-nuclei appears to be strongly anticorrelated with their rate of photodisintegration.

immediately struck by the high degree of anticorrelation shown by the two curves. Abundances are high for nuclei that have smaller photodisintegration rates, i.e., longer lifetimes. The abundances decrease systematically with increasing atomic number, while Λ for the p-nuclei increases. Particularly strong anticorrelation occurs in the vicinity of closed nuclear shells as denoted by arrows in the figure.

What quantitative meaning can one assign to this anticorrelation? If all the p-nuclei were made at one temperature by a flow that had achieved a steady state all the way from lead to iron, then all products $N_{\odot}\Lambda$ would be equal to the same constant and Λ and $N_{\odot}$ would be anticorrelated as shown. However, the large range in Λ makes it apparent that this could not have happened. Any photon exposure sufficient to create a steady-state flow in the vicinity of ^{92}Mo, for example, would completely destroy all the heavy p-nuclei. The more proper interpretation of Figure 2 leads us to think in terms of a *distribution* of exposure strengths. Such a restriction is similar to the distribution of neutron exposure strengths required for producing the solar abundances of the s-process nuclei. We can understand the results in terms of the following prescription for generating the p-nuclei. For simplicity first consider a calculation where the temperature is held constant. After some short period of time $t_H \approx 1/\Lambda_H$, where Λ_H is a typical photodisintegration rate for heavy nuclei, the heavy p-nuclei will achieve a steady state. Take a snapshot of their abundances. Allow further time to elapse, say $t_M \approx 1/\Lambda_M$, where M stands for medium-weight nuclei. Take another snapshot. Finally, allow the lightest p-nuclei to achieve steady state and take a final snapshot. The sum of the snapshots will have $N_{\odot}\Lambda$ roughly equal to a constant and will resemble the abundance curve in Figure 2, even though not all nuclei were synthesized together in one steady-state flow. A more realistic but analogous picture would involve, instead of a distribution of time scales at constant temperature, a distribution of exposure temperatures all occurring for roughly the same time scale. This is the approach we shall adopt in the next section.

It is important, however, to clarify at this point what might appear to be a logical inconsistency in Figure 2 and in our discussion thus far, namely that Λ *increases* for nuclei of increasing nuclear charge. The quantity Λ is dominated in many cases by $\lambda_{\gamma\alpha}$, which one would think must *decrease* with nuclear charge because of the increasing Coulomb barrier. Certainly $\lambda_{\alpha\gamma}$ decreases dramatically as one proceeds from $Z = 40$ to $Z = 82$. Why doesn't $\lambda_{\gamma\alpha}$, which is related to $\lambda_{\alpha\gamma}$ by reciprocity theorems, also decrease? The answer is that in general $\lambda_{\gamma\alpha}$ *does* show such a decrease, but we are not looking at the general case. We are examining nuclei that satisfy equation (5) and as a result are typified by relatively small and, in fact, frequently negative values of S_α. It turns out that for nuclei that obey equation (5) the quantity S_α decreases with increasing atomic number at a rate sufficient to balance and, in fact, overcome the effect of the increasing Coulomb barrier (see eq. [4]). As a result $\lambda_{\gamma\alpha}$ for the nuclei at branching points actually increases as we go to heavier and heavier species. This is very important. Were it not for the fact that the nuclear systematics are such as to make Λ an increasing function of A, not only would we lose the suggestive picture shown in Figure 2, but synthesis of the p-nuclei in the way we are describing would be impossible. If Λ decreased for the larger masses under consideration, then any flux sufficient to destroy lead would also destroy the products of lead's photodisintegration, and so on down to iron. No nucleosynthesis of intermediate-weight nuclei could occur. Fortunately, the nuclear systematics are what they are and the γ-process can proceed stepwise as described.

b) *Results of Numerical Calculations*

We now move from the qualitative considerations of the previous section to a numerical treatment of the nucleosynthesis expected from the γ-process for specific values of temperature and time scale. As in explosive nucleosynthesis calculations of the past (e.g., Woosley, Arnett, and Clayton 1973, henceforth WAC), we parametrize the explosion by a peak value of temperature, T_{9m}, that decays away exponentially with time. That is,

$$T_9(t) = T_{9m} \exp(-t/\tau_T)\,. \tag{6}$$

Traditionally it has been assumed that the explosive expansion would be adiabatic and would take place on a hydrodynamic time scale. Then τ_T is related to the local density at the peak of the explosion, ρ_m, by

$$\tau_T = 3\tau_{\rm HD} = 3/(24\pi G\rho_m)^{1/2} = 1338\rho_m{}^{-1/2}\ {\rm s}\,. \tag{7}$$

From the previous works of AT and B^{2}FH one may anticipate that temperatures at least as high as $T_9 = 2$ are required to produce significant transmutation of the heavy elements by (γ, n) reaction for any realistic value of explosion time scale. Synthesis of lighter elements like ^{92}Mo by photodisintegration will require still larger values of temperature. Such temperatures are suggestive of those zones in supernovae which experience explosive carbon or oxygen burning (Arnett 1969; WAC). Arguments based upon nucleosynthesis and presupernova structure yield a range of densities of roughly $\rho_m \approx 10^5$–10^7 g cm^{-3} for such zones, from which we deduce $\tau_T \approx 1$ s. We also note that such densities would relax the severe energetic constraints discussed for the more traditional p-process (see § II*a*).

In all that follows we will adopt $\tau_T = 1$ s as a working hypothesis regardless of the exact value of peak photon temperature assumed. The current knowledge of supernova structure and evolution is sufficiently uncertain that that parametrization is as accurate as any other we might care to make at the present time. This simple approximation has the advantage of decoupling the treatment of the γ-process from an exact specification of its site. Thus, while we feel that explosive carbon and oxygen burning form the most reasonable context for our calculations, the occurrence of the γ-process may not be limited to specifically those stellar zones. Clearly, other combinations of temperature and time scale will yield results similar to those we are about to derive, but the following calculations should be illustrative.

In order to follow the nucleosynthesis that occurs by the γ-process, a large reaction network containing over 1000 nuclei from germanium to bismuth was constructed. The boundaries of the network, given in Table 3, were chosen so as to include all possible seed nuclei and to allow sufficient excursion into the proton-rich region of the periodic chart that charged-particle emission would surely occur. Since it is possible for photodisintegration processes involving the heavy nuclei near Pb to play a role in enhancing the p-nuclei in the lighter mass region ($A \approx 110$), it is essential that all seed and p-nuclei be included in one network. The species contained within the boundaries given in Table 3 were coupled together by all reaction links involving a photon in the entrance channel, and the resulting system of differential equations evolved using the techniques discussed in Appendix B. Weak interactions were ignored because of the short time scale involved and because the expected path of photodisintegration lies near the valley of beta stability. For initial composition in this first series of calculations, a solar-system distribution (Cameron 1973) of nuclei in the mass range $70 \leq A \leq 209$ was employed (a nonsolar seed distribution will be considered in § III*d*). This composition was exposed to a radiation bath having a temperature history given by equations (6) and (7) for a range of peak temperatures of $2.1 \leq T_{9m} \leq 3.2$. The results of these calculations are given in Table 4. For each peak explosion temperature the results are expressed in terms of a ratio to the solar values given in Table 1. The entry "120" for ^{158}Dy under the column $T_{9m} = 2.5$ shows, for example, that in an explosive evolution starting from a peak temperature $T_{9m} = 2.5$ and cooling exponentially to a temperature $T_9 = 0.9$ in 1 second, sufficient r- and s-process seeds are converted into ^{158}Dy and proton-rich progenitors of ^{158}Dy to produce a mass fraction of 1.49×10^{-10} of ^{158}Dy or 120 times its initial (solar) value. Entries in italics indicate that at the value of explosion temperature given, the species is synthesized predominantly as a proton-rich progenitor (usually $[Z + 2, A]$). The number "1" shows that no modification of the initial abundance occurs, and blank entries are given when the final abundance is less than 10% of the initial abundance.

The small values for ^{113}In, ^{115}Sn, ^{138}La, and ^{180}Ta emphasize the difficulty of synthesizing an odd-particle nucleus or, even worse, an odd nucleus by photodisintegration processes at any temperature. Destruction of such nuclei by photonuclear processes occurs too rapidly for a sizable abundance to ever accumulate. One must therefore look elsewhere in nature for the synthesis of such species. This is a shortcoming which our theory shares with those such as AT which are based on synthesis in hydrogen zones. The species ^{113}In and ^{115}Sn are probably made by a branch of the s-process (see Table 1). The rare species ^{138}La and ^{180}Ta may be produced by spallation (Audouze 1970; Hainebach, Schramm, and Blake 1976).

Also given in Table 4 are entries for three p-nuclei that may exist in the solar system as extinct or nearly extinct radioactivities, ^{92}Nb, ^{146}Sm, and ^{202}Pb. Since solar-abundance data are not available for these

TABLE 3

NUCLEAR REACTION NETWORK FOR THE γ-PROCESS (1083 Isotopes)

Element	Z	A_{min}	A_{max}	Element	Z	A_{min}	A_{max}
Ge........	32	68	78	Ce.........	58	126	148
As.........	33	70	81	Pr.........	59	127	150
Se.........	34	71	84	Nd.........	60	132	152
Br.........	35	74	87	Pm........	61	133	154
Kr........	36	75	90	Sm........	62	136	156
Rb........	37	80	93	Eu.........	63	137	159
Sr.........	38	82	95	Gd........	64	140	162
Y.........	39	84	97	Tb.........	65	143	164
Zr.........	40	86	100	Dy........	66	148	166
Nb........	41	88	102	Ho........	67	149	169
Mo........	42	89	104	Er.........	68	151	173
Tc.........	43	92	106	Tm........	69	152	176
Ru........	44	94	108	Yb........	70	154	178
Rh........	45	96	110	Lu.........	71	156	180
Pd.........	46	98	112	Hf.........	72	158	183
Ag........	47	100	116	Ta.........	73	164	186
Cd........	48	102	119	W.........	74	166	189
In.........	49	103	124	Re.........	75	168	191
Sn.........	50	105	128	Os.........	76	170	195
Sb.........	51	106	132	Ir.........	77	172	198
Te.........	52	108	135	Pt.........	78	174	201
I..........	53	114	137	Au.........	79	178	204
Xe.........	54	116	140	Hg........	80	180	206
Cs.........	55	117	142	Tl.........	81	188	208
Ba.........	56	120	144	Pb.........	82	190	208
La.........	57	121	146	Bi.........	83	192	209

TABLE 4

OVERPRODUCTION FACTORS* FOR *p*-NUCLEI AT VARIOUS EXPLOSION TEMPERATURES (solar seed)

Species	Temperature											
	2.1	2.2	2.3	2.4	2.5	2.6	2.7	2.8	2.9	3.0	3.1	3.2
^{196}Hg	4.5	54.	440.	300.	*1500.*	*340.*	...	...	...	...	...	...
[^{202}Pb/^{196}Hg]†	1.5	5.7	4.4	1.5	2.8(−2)	...	...	...	...	...	...	...
^{190}Pt	1.6	26.	1100.	3500.	*1500.*	*1800.*	...	...	...	...	...	...
^{184}Os	6.4	290.	2900.	500.	*150.*	*72.*	...	...	...	...	...	...
^{180}W	130.	580.	170.	*1400.*	*1100.*	*490.*	...	...	...	...	...	...
^{180}Ta	49.	1.	...	...	...	...	...	...	...	...	...	...
^{174}Hf	35.	360.	420.	*150.*	*590.*	*310.*	...	...	...	...	...	...
^{168}Yb	3.4	55.	530.	420.	*640.*	*4400.*	*41.*	...	...	...	...	...
^{164}Er	1.6	9.3	41.	17.	*43.*	*760.*	*160.*	...	...	...	...	...
^{162}Er	1.0	2.3	63.	490.	250.	*380.*	*81.*	...	...	...	...	...
^{158}Dy	2.1	22.	320.	810.	120.	*270.*	*100.*	...	...	...	...	...
^{156}Dy	1.0	1.1	13.	400.	1300.	380.	170.	...	...	...	...	...
[^{146}Sm/^{144}Sm]†	4.2	3.0	1.7	1.5(−1)	1.2(−2)	*2.4(−2)*	*3.0(−2)*	*2.3(−2)*	*2.8(−4)*	...	...	...
^{144}Sm	1.0	1.1	2.2	13.	48.	160.	1100.	1200.	680.	59.	...	...
^{152}Gd	1.2	3.5	30.	91.	1.8	0.5	0.2	...	...	...	...	...
^{138}La	1.0	1.2	1.4	1.4	0.9	0.1	...	...	...	...	...	...
^{138}Ce	1.0	1.0	1.2	3.8	21.	86.	96.	*100.*	*155.*	*38.*	...	...
^{136}Ce	1.0	1.0	1.0	1.0	2.0	29.	40.	23.	*30.*	*7.6*	...	...
^{132}Ba	1.0	1.0	1.1	2.1	13.	190.	560.	*82.*	*92.*	*37.*	...	...
^{130}Ba	1.0	1.0	1.0	1.0	1.1	13.	290.	120.	23.	8.6	...	...
^{130}Xe‡	5.7	6.1	6.1	6.6	9.5	7.0	0.1	...	...	...	...	...
^{128}Xe‡	11.	14.	14.	14.	16.	26.	16.	*23.*	*4.8*	*2.0*	...	...
^{126}Xe	1.0	1.0	1.2	2.7	14.	120.	590.	410.	*42.*	*18.*	...	...
^{124}Xe	1.0	1.0	1.0	1.0	1.0	3.2	76.	270.	38.	15.	...	...
^{120}Te	1.0	1.0	1.0	1.1	1.6	9.8	220.	530.	66.	15.	...	...
^{115}Sn	1.0	0.9	0.7	0.1	...	...	...	...	...	...	...	...
^{114}Sn	1.0	1.0	1.2	1.5	1.7	2.9	14.	200.	690.	360.	3.5	...
^{112}Sn	1.0	1.0	1.0	1.0	1.0	1.0	1.1	9.9	140.	320.	16.	...
^{113}In	1.0	1.0	1.0	1.2	2.0	6.0	15.	8.1	0.5	0.2	...	...
^{108}Cd	1.0	1.0	1.0	1.0	1.3	3.2	20.	70.	36.	120.	8.	...
^{106}Cd	1.0	1.0	1.0	1.0	1.0	1.0	1.6	15.	63.	290.	61.	...
^{102}Pd	1.0	1.0	1.0	1.0	1.2	2.8	18.	83.	86.	160.	65.	...
^{98}Ru	1.0	1.4	3.1	6.9	8.1	10.	27.	45.	15.	8.2	6.4	...
^{96}Ru	1.0	1.0	1.0	1.0	1.0	1.0	1.1	3.5	5.4	5.1	4.4	...
[^{92}Nb/^{92}Mo]†	7.5(−5)	7.6(−4)	6.2(−3)	3.4(−2)	6.6(−2)	3.4(−2)	1.1(−3)	...	...	...	...	...
^{94}Mo	1.0	1.1	1.4	2.4	2.9	4.0	6.2	2.4	0.2	0.1	0.1	...
^{92}Mo	1.0	1.0	1.0	1.0	1.0	1.0	1.6	3.9	5.7	4.9	7.6	...
^{84}Sr	1.0	1.0	1.0	1.0	1.0	1.0	1.0	1.0	1.3	3.1	14.	85.
^{80}Kr‡	1.0	1.0	1.0	1.0	1.0	1.0	1.0	1.1	2.0	8.5	32.	34.
^{78}Kr	1.0	1.0	1.0	1.0	1.0	1.0	1.0	1.0	1.0	1.2	7.0	17.
^{76}Se‡	1.0	1.1	1.3	1.8	1.8	1.8	1.9	1.9	2.6	5.2	7.7	2.7
^{74}Se	1.0	1.0	1.0	1.0	1.0	1.0	1.0	1.1	1.4	4.4	17.	11.

* Relative to solar (Cameron 1973) abundances. Entries in italics are dominantly the radioactive progenitor ($Z + 2$, A).

† Bracketed ratios give production of long-lived unstable isotope relative to stable *p*-nucleus.

‡ *s*-process nucleus with interesting γ-process contribution or modification.

nuclei, we express their production in terms of a ratio relative to some neighboring isotope produced by the γ-process. Thus the production of ^{146}Sm is expressed as a ratio relative to ^{144}Sm, and ^{92}Nb is expressed relative to ^{92}Mo. We note in passing that the production for ^{146}Sm/^{144}Sm never exceeds a few percent in zones where significant amounts of ^{144}Sm are synthesized, a result that differs qualitatively from that of AT. The nucleus ^{146}Sm has been proposed as a possible *p*-process cosmochronometer (Audouze and Schramm 1972; AT). This possibility, which seems to us to be relatively remote, will be discussed in greater detail in § V.

We also include in Table 4 two nuclei the bulk of whose solar abundance is almost certainly *not* attributable to the *p*-process (or γ-process). These are the species ^{128}Xe and ^{130}Xe. Clayton (1976) has pointed out that the *p*-process contribution to these isotopes may be important for understanding the origin of so-called carbonaceous chondrite fission xenon (Reynolds and Turner 1964; Manuel, Hennecke, and Sabu 1972; Lewis, Srinivasan, and Anders 1975).

It is readily apparent from inspection of Table 4 that no single temperature exposure can possibly produce all of the *p*-nuclei if a constant time scale is assumed, a result that is expected from the qualitative considerations of the previous section. One must sum a distribution of exposures in order to obtain even an approximate representation of the solar abundances. This requirement reflects the reality of the astrophysical situation. It is not reasonable that all zones in all supernovae that reach peak temperatures in the vicinity of 2–3 × 10^9 K should reach some unique value. Instead, any real supernova will exhibit a range of conditions, a range that will be further broadened by consideration of the variety of supernova masses in the Galaxy's history. Furthermore, it is important to note that the temperature–time step combination used to generate Table 4 is not unique. For example, we have found that very similar results are obtained if a time scale 100 times longer is employed and the peak temperature scale is shifted downward by 2 × 10^8 K. Similar arguments have been proposed by Michaud and Fowler (1972) to account for a range of peak temperatures in silicon burning. The problem, of course, is to know what distribution of exposure strengths has actually occurred.

c) *Results Averaged over Peak Temperatures*

In order to compute the proper summation of the abundance vectors in Table 4, the characteristics of the site of γ-process synthesis must be specified. Let the total synthesis from the γ-process be given by the summation

$$N_{\mathrm{tot}}(Z, A) = \sum_i C_i N_i(Z, A) , \tag{8}$$

where C_i is some weighting function subject to the condition $\sum_i C_i = 1$ and $N_i(Z, A)$ denotes the nucleosynthesis vector resulting from expansion from the ith value of T_{9m}. The C_i are functions of both the preexplosive evolution of the typical supernova and explosion characteristics which we cannot hope to specify at the present time. For illustrative purposes we have prepared "case A" in Table 5 which shows the values of $N_{\mathrm{tot}}(Z, A)$ relative to solar abundances that result in the simplest possible case where each temperature contributes equally, i.e., $C_i = 1/12$ for all "i." These results are also displayed graphically in Figure 3*a* for those stable elements which are generally attributed to the *p*-process. Even this simplest case is impressive. All *p*-nuclei heavier than $A = 110$ except for ^{113}In, ^{115}Sn, ^{138}La, ^{152}Gd, and ^{180}Ta are consistently coproduced within a factor of 5 of their solar abundance (i.e., relative to the mean overproduction factor). Most are within a factor of 3. Isotopic ratios are especially well reproduced. Those five nuclei that are underproduced are likely to be synthesized by either the *s*-process (^{113}In, ^{115}Sn, and ^{152}Gd) or by spallation (^{138}La and ^{180}Ta). Considering the many uncertainties inherent in the simple model represented by case A, this is a resounding success for the theory! Below mass number 110, however, the situation is not so encouraging. Many *p*-nuclei are consistently produced relative to one another, but the average overproduction factor is at least an order of magnitude less than that value which typifies the production of *p*-nuclei heavier than $A = 110$. How is this to be explained?

d) *Nonsolar Seed and Nonlinear Temperature Distributions*

One possible explanation for the deficient production of $A \leq 110$ *p*-nuclei is that we have erred greatly in assuming a seed distribution for the γ-process that is initially solar. Although this assumption may not be the sole cause underlying all the deficiencies in case A of Table 5, it is certainly an erroneous one! Prior to exploding, the stellar zones under consideration

TABLE 5

OVERPRODUCTION FACTORS* FOR *p*-NUCLEI AVERAGED OVER TEMPERATURE

Species	Case A	Case B	Species	Case A	Case B
^{196}Hg	220.	690.	^{126}Xe	100.	180.
[^{202}Pb/^{196}Hg]†	1.2	1.1	^{124}Xe	34.	75.
^{190}Pt	660.	1000.	^{120}Te	71.	99.
^{184}Os	320.	460.	[^{115}Sn]†	0.2	0.4
^{180}W	320.	660.	^{114}Sn	110.	260.
[^{180}Ta]†	4.2	14.	^{112}Sn	41.	99.
^{174}Hf	160.	310.	[^{113}In]†	3.0	5.7
^{168}Yb	500.	1100.	^{108}Cd	22.	66.
^{164}Er	86.	160.	^{106}Cd	36.	99.
^{162}Er	110.	170.	^{102}Pd	35.	110.
^{158}Dy	140.	260.	^{98}Ru	11.	22.
^{156}Dy	190.	340.	^{96}Ru	2.1	4.4
[^{146}Sm/^{144}Sm]†	2.4(−2)	2.3(−2)	[^{92}Nb/^{92}Mo]†	4.8(−3)	2.1(−3)
^{144}Sm	270.	540.	^{94}Mo	1.8	5.0
[^{152}Gd]†	11.	15.	^{92}Mo	2.5	5.9
[^{138}La]†	0.5	2.1	^{84}Sr	9.3	290.
^{138}Ce	42.	160.	[^{80}Kr]†	7.1	100.
^{136}Ce	20.	93.	^{78}Kr	2.8	32.
^{132}Ba	82.	300.	[^{76}Se]†	2.6	100.
^{130}Ba	38.	140.	^{74}Se	3.5	77.
[^{130}Xe]†	3.4	6.8	Mean†	120.	260.
[^{128}Xe]†	12.	18.			

* Relative to Cameron 1973.

† Bracketed species not included in calculation of mean.

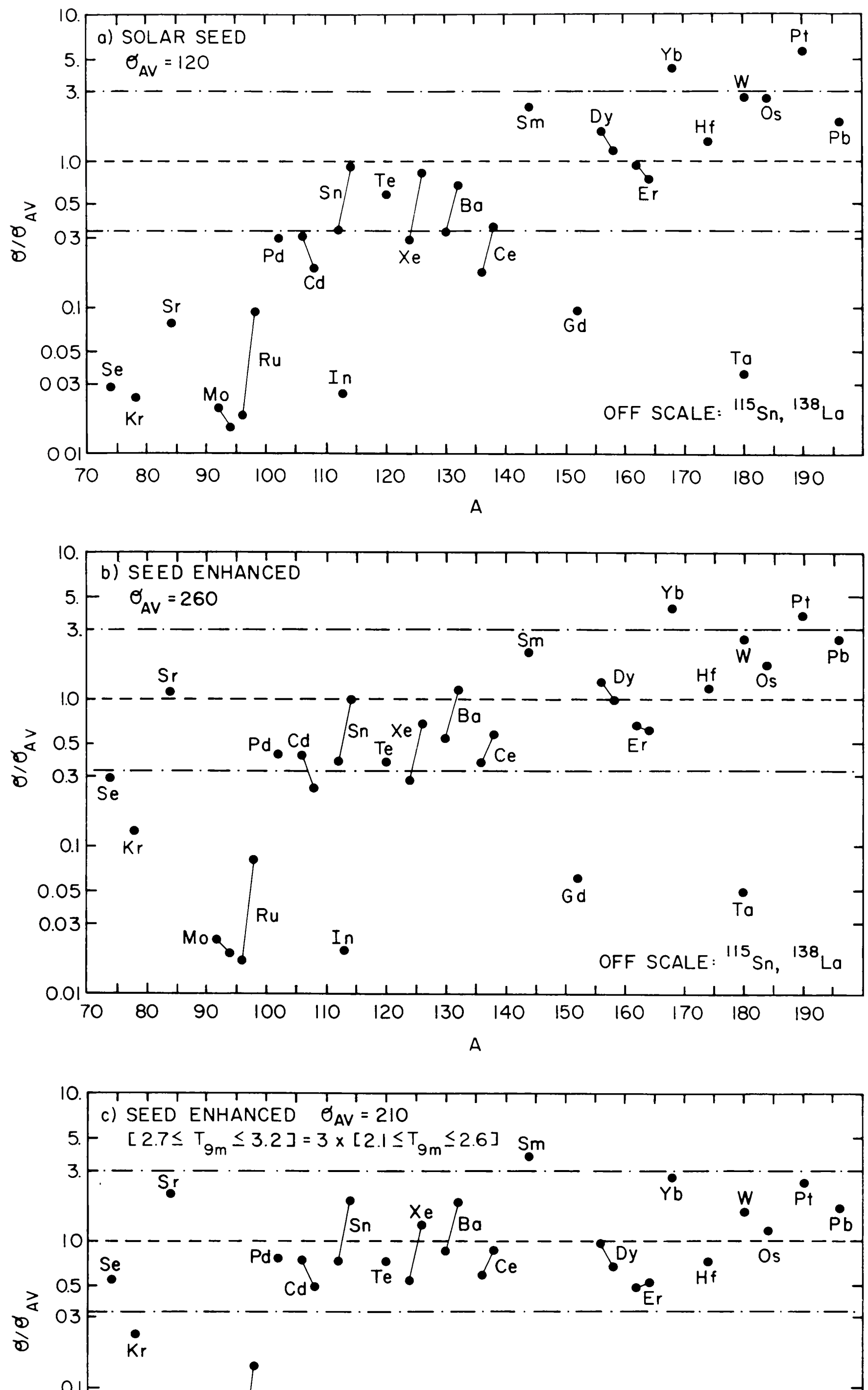

FIG. 3.—Relative overproduction factors for the p-nuclei as a function of atomic weight A. Lines connect isotopes of the same element. (a), Results for an initial solar distribution of heavy elements and all temperatures weighted evenly. (b), Results for an s-process enhanced distribution of heavy elements with all temperatures weighted evenly. (c), Results for an s-process enhanced distribution of heavy elements, but with the contribution from higher temperatures weighted 3 times more than that from lower temperatures.

have experienced hydrostatic helium burning and perhaps carbon burning as well. They are therefore almost certain to be enriched in s-process seeds that have very nonsolar abundances. Couch, Schmiedekamp, and Arnett (1974) and Lamb *et al.* (1977) have studied the s-process that occurs during core helium burning in massive stars. Both studies yielded a very nonsolar pattern of s-nuclei characterized by large overproductions of light elements and smaller enhancements of heavier ones. In the work by Couch, Schmiedekamp, and Arnett (1974), which employed as initial seed only iron and lighter elements, overproductions of roughly a factor of 50 occurred for elements up to $A \approx 90$. These were accompanied by essentially no production of heavier nuclei. Lamb *et al.* (1977), using as seed a Population I mixture of *all* nuclei up to and including lead, also found a similar enhancement of $A \leqslant 90$ nuclei. In addition they found a rearrangement of heavy nuclei that yielded significant enhancements of isotopes with $A > 90$. The abundances of these heavy nuclei were increased by highly variant factors the mean of which was roughly 3. Since the γ-process always synthesizes p-nuclei exclusively from those isotopes which are heavier than the p-nucleus itself, a systematic enhancement of lighter seed nuclei will selectively increase the production of still lighter p-nuclei. Thus use of the actual seed distribution following stellar helium burning should yield improved results as compared to those in case A of Table 5.

TABLE 6

OVERPRODUCTION FACTORS* FOR p-NUCLEI AT VARIOUS EXPLOSION TEMPERATURES (Enhanced seed)

Species	Temperature											
	2.1	2.2	2.3	2.4	2.5	2.6	2.7	2.8	2.9	3.0	3.1	3.2
^{196}Hg	10.	180.	1700.	1100.	*4300.*	*940.*	...	...	...	...	...	...
[^{202}Pb/^{196}Hg]†	5.0	6.9	3.6	1.0	2.4(−2)	8.3(−6)	...	...	...	...	...	...
^{190}Pt	4.5	44.	750.	2000.	*4700.*	*5100.*	...	...	...	...	...	...
^{184}Os	43.	640.	4100.	370.	*190.*	*190.*	...	...	...	...	...	...
^{180}W	610.	2500.	550.	*1800.*	*1100.*	*1300.*	...	...	...	...	...	...
^{180}Ta	170.	3.3	...	...	...	...	...	...	...	...	...	...
^{174}Hf	74.	870.	980.	*330.*	*600.*	*840.*	...	...	...	...	...	...
^{168}Yb	12.	210.	1700.	1300.	*1000.*	*8900.*	*90.*	...	...	...	...	...
^{164}Er	1.8	14.	63.	28.	*100.*	*1400.*	*360.*	...	...	...	...	...
^{162}Er	1.0	2.8	100.	760.	390.	*660.*	*170.*	...	...	...	...	...
^{158}Dy	2.9	38.	620.	1500.	220.	*460.*	*220.*	...	...	...	...	...
^{156}Dy	1.0	1.1	25.	750.	2400.	560.	370.	...	...	...	...	...
[^{146}Sm/^{144}Sm]	4.7	6.7	2.3	9.9(−1)	1.1(−2)	*2.2(−2)*	*3.0(−2)*	*2.2(−2)*	*2.3(−4)*	...	...	...
^{144}Sm	1.0	1.1	5.0	30.	88.	280.	2200.	2400.	1400.	112.	...	...
^{152}Gd	2.7	5.1	40.	130.	3.2	0.7	0.4	...	...	...	...	...
^{138}La	1.5	4.5	7.1	7.0	4.4	0.5	...	...	...	...	...	...
^{138}Ce	1.0	1.0	2.1	17.	120.	500.	510.	*300.*	*330.*	*74.*	...	...
^{136}Ce	1.0	1.0	1.0	1.1	6.8	170.	790.	73.	62.	14.	...	...
^{132}Ba	1.0	1.0	1.4	4.2	37.	680.	2100.	*400.*	*250.*	*69.*	...	...
^{130}Ba	1.0	1.0	1.0	1.0	1.4	43.	1100.	480.	63.	17.	...	...
^{130}Xe‡	11.	11.	11.	13.	20.	15.	0.2	...	...	...	...	...
^{128}Xe‡	7.1	7.5	7.6	8.1	13.	39.	35.	*88.*	*16.*	*4.0*	...	...
^{126}Xe	1.0	1.0	1.1	1.9	9.8	140.	930.	940.	*140.*	*33.*	...	...
^{124}Xe	1.0	1.0	1.0	1.0	1.0	3.3	120.	610.	130.	29.	...	...
^{120}Te	1.0	1.0	1.0	1.4	3.8	23.	280.	660.	190.	27.	...	...
^{115}Sn	1.0	0.9	0.7	0.2	0.1	0.1	0.2	0.2	0.1	...	...	...
^{114}Sn	1.0	1.0	1.2	1.6	2.4	7.6	47.	480.	1700.	830.	7.3	...
^{112}Sn	1.0	1.0	1.0	1.0	1.0	1.0	1.3	23.	350.	770.	35.	...
^{113}In	1.0	1.0	1.0	1.3	3.2	12.	31.	17.	1.0	0.4	...	...
^{108}Cd	1.0	1.0	1.0	1.2	2.6	13.	86.	270.	110.	290.	18.	...
^{106}Cd	1.0	1.0	1.0	1.0	1.0	1.1	3.6	59.	230.	750.	140.	...
^{102}Pd	1.0	1.0	1.0	1.1	1.9	8.4	67.	310.	320.	430.	150.	...
^{98}Ru	1.1	1.4	3.2	7.0	8.8	16.	54.	92.	36.	24.	15.	...
^{96}Ru	1.0	1.0	1.0	1.0	1.0	1.0	1.4	6.7	14.	15.	9.8	...
[^{92}Nb/^{92}Mo]	7.5(−5)	7.8(−4)	6.4(−3)	3.4(−2)	7.0(−2)	3.2(−2)	5.6(−4)	...	...	...	...	...
^{94}Mo	1.0	1.2	2.0	4.1	6.0	12.	23.	8.9	0.5	0.4	0.3	...
^{92}Mo	1.0	1.0	1.0	1.0	1.0	1.1	3.0	12.	17.	15.	18.	...
^{84}Sr	1.0	1.0	1.0	1.0	1.0	1.0	1.1	3.3	21.	120.	620.	2700.
^{80}Kr‡	1.0	1.0	1.0	1.0	1.0	1.1	1.6	4.8	24.	146.	515.	550.
^{78}Kr	1.0	1.0	1.0	1.0	1.0	1.0	1.0	1.0	1.2	8.3	110.	260.
^{76}Se‡	73.	75.	81.	92.	94.	94.	94.	96.	110.	170.	210.	58.
^{74}Se	1.0	1.0	1.0	1.0	1.0	1.1	1.8	6.0	28.	150.	490.	240.

* Relative to solar (Cameron 1973) abundances. Entries that are italicized are dominantly the radioactive progenitor ($Z + 2,A$).

† Bracketed ratios give production of long-lived unstable isotope to stable p-nucleus.

‡ s-process nucleus with interesting γ-process modification. The production ratio given here includes the preexplosive enhancement from helium burning (Lamb *et al.* 1977).

To test the hypothesis, we have repeated the calculations discussed in § III*b* using the modified seed distribution of Lamb *et al.* (1977) for a 25 $M_\odot$ star. The results are displayed in Table 6, which has a format similar to Table 4. The nucleosynthesis averaged over peak exposure temperature is also given as case B in Table 5 and in Figure 3*b*. The synthesis of heavy nuclei, $A \geqslant 110$, is very similar to that obtained with solar seed (case A and Fig. 3*a*) except for an overall increase of roughly a factor of 2 reflecting the increased amount of heavy seed available. For the lightest *p*-nuclei, ^{74}Se, ^{78}Kr, and ^{84}Sr, there is a much larger increase due to the nature of the seed distribution.

While the Lamb *et al.* seed abundances certainly yield an overall improvement in the production of *p*-nuclei, the situation is still far from completely satisfying. One must still contend with disappointingly small syntheses of species of intermediate mass like ^{92}Mo, ^{94}Mo, ^{96}Ru, and ^{98}Ru. We feel that all four of these species must be produced by a γ- or *p*-process. What is the explanation? A possibility to be briefly explored is that the peak temperature distribution is nonlinear, i.e., that the C_i in equation (8) are not all equal. Examination of Tables 4 and 6 shows that the maximum production of the light nuclei occurs for higher explosion temperatures than those which make $A \geqslant 110$. Thus a weighting of the temperature distribution function toward higher values will tend to selectively enhance the lighter *p*-nuclei. We have prepared Figure 3*c* to illustrate this effect. This figure employed $C_i = 1/24$ for $2.1 \leq T_{9m} \leq 2.6$ and $C_i = 3/24$ for $2.7 \leq T_{9m} \leq 3.2$. Admittedly this choice of peak temperature distribution is completely ad hoc but it does illustrate two important points: (1) a nonlinear peak temperature exposure distribution can correct for the overall "skewed" production of $A \leqslant 110$ and $A > 110$ *p*-nuclei, as evidenced in Figure 3*b*, but (2) it *cannot* substantially increase the overall production of Ru and Mo isotopes. There simply is no temperature in Table 6 where Mo and Ru production dominates. The Mo and Ru *p*-nuclei are too abundant and there is insufficient seed of atomic weight $A > 96$ to ever lead to large overproduction factors for these species.

It follows that all likely models for the synthesis of ^{92,94}Mo and ^{96,98}Ru must involve the propagation of additional seed material up from below $A = 92$ either prior to or during the explosive disruption. This could occur in one of two ways: (1) additional preexplosive *s*-processing, or (2) particle-induced reactions during the explosion. Because of its comparative simplicity we favor the former of these two explanations (certainly not an overwhelming argument! See § IV for more detailed discussion.) Helium burning will be followed by carbon burning and additional *s*-processing will occur (Arnett and Truran 1969). The question of how much processing depends sensitively on unknown stellar parameters, but it is likely that the resultant seed distribution would have large enhancements not only of $A \leqslant 90$ but also of $90 \leqslant A \leqslant 140$ (i.e., out to the vicinity of barium). This additional seed, upon photodisintegration, might fill in the gaps at molybdenum and ruthenium. Such a scenario would require that the site of the γ-process be those zones of supernovae that experienced hydrogen, helium, and carbon burning prior to their disruption. The γ-process then becomes a variant of low-temperature "explosive oxygen burning." As the next section will show, this picture has additional attractive features.

IV. EFFECT OF BACKGROUND PARTICLE FLUXES

Thus far it has been implicitly assumed that the γ-process can be decoupled from all other nuclear burning processes that occur in those exploding stellar zones achieving $T = 2\text{–}3 \times 10^9$ K. Presumably these processes involve either the explosive burning of carbon (Arnett 1969) or oxygen (Truran and Arnett 1970; WAC). In one sense such a "perturbation" approach is clearly valid. The particles released and photons absorbed by the γ-process are so few compared to the source and sink terms in the dominant burning process that they certainly have negligible effect upon the background abundances of these species. However, the effects of the free-particle abundances themselves, the neutrons, protons, and α-particles that are present during carbon or oxygen burning may alter the character of the γ-process, and must be considered.

Besides photons themselves, the most important exposures during the γ-process involve neutrons and protons. The presence of these nucleons acts to restrict flows toward proton-rich nuclei and nuclei of lower Z, respectively. While the actual flux history of these particles is sensitive to unknown composition and explosion parameters, it is possible to obtain representative values by employing the same simple characterization of explosion thermodynamics given in equations (6) and (7). In addition one assumes that the explosion is adiabatic so that $\rho_b \propto T_9{}^3$. The results of four such mock explosions are shown in Figures 4*a* and 4*b*. These curves were obtained by using reaction networks similar to those of Arnett (1969) and WAC to track the nuclear evolution of zones expanding from $\rho = 5 \times 10^5$ g cm^{-3} and peak temperatures $T_{9m} = 2.5$ and 3.0. The time scale for an *e*-fold decrease in temperature was 1 second in all cases, but two different initial compositions were employed. One composition, typical of a helium-exhausted zone, was by mass 50% ^{12}C, 48% ^{16}O, and 2% ^{22}Ne. The other, typical of a carbon-exhausted zone, was 54% ^{16}O, 28% ^{24}Mg, 2% ^{26}Mg, and 14% ^{28}Si.

The choice of composition turns out to be a key factor in describing the character of the γ-process. As Figure 4*a* shows, the neutron flux that results from oxygen burning at $T_9 = 2.5$ is roughly seven orders of magnitude smaller than results from carbon burning under identical conditions. This large difference results from a similar ratio in the reaction rates for ^{12}C + ^{12}C and ^{16}O + ^{16}O. Since carbon burning at $T_9 = 2.5$ produces α-particles $\sim 10^7$ times faster, the rate of the

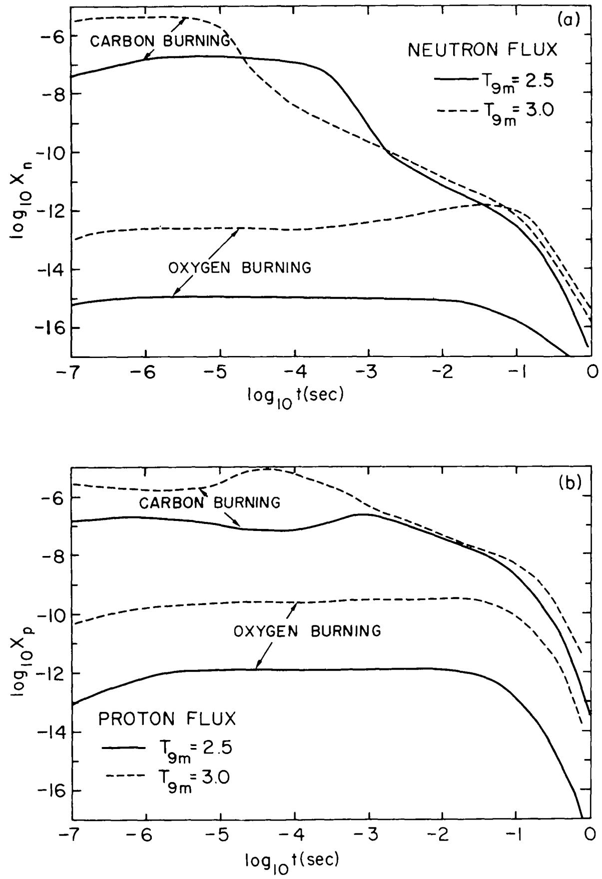

FIG. 4.—Neutron (*a*) and proton (*b*) mass fractions as a function of time during explosive oxygen and carbon burning for the peak temperatures $T_{9m} = 2.5$ and 3.0.

^{22}Ne (α, n) ^{25}Mg reaction during carbon burning is $\sim 10^7$ times more rapid than the ^{26}Mg (α, n) ^{29}Si reaction during oxygen burning [the cross section factors for the (α, n) reactions themselves do not differ markedly at this temperature]. These are the dominant neutron sources during carbon and oxygen burning, and the difference is reflected in the free neutron abundances.

In order to significantly modify the γ-process, this neutron flux must be sufficient to impede (γ, n) reactions for some nucleus short of the branch points listed in Table 2. Since the slowest (γ, n) rate short of the branch point (Z, A_{branch}) characteristically occurs at $(Z, A_{\text{branch}} + 2)$, a rough criterion for the neutrons being important is

$$\rho X_n \lambda_{n\gamma}(A_{\text{branch}} + 1) \gtrsim \text{Max}\,[1/\Delta t, \lambda_{\gamma n}(A_{\text{branch}} + 2)]\,, \tag{9}$$

where the quantities $\lambda_{n\gamma}$ and $\lambda_{\gamma n}$ are defined in Appendix A and Δt is a typical time scale for the duration of neutron mass fraction X_n. Adopting the representative values $\rho = 5 \times 10^5$ g cm^{-3} and $\lambda_{n\gamma} \approx 3 \times 10^7$ cm^3 mole^{-1} s^{-1} (to an order of magnitude), this condition becomes

$$(X_n/10^{-13}) \gtrsim \text{Max}\,[1/\Delta t, \lambda_{\gamma n}(A_{\text{branch}} + 2)]\,. \tag{10}$$

Examination of the rates in Table 7 and values of X_n in Figure 4*a* shows that this criterion is not satisfied for any element during explosive oxygen burning at $T_{9m} \leq 2.5$. For higher values of peak explosion temperature, $T_{9m} = 3.2$ for example, some hindrance of flow may occur, but only for (γ, n) reactions involving the very lightest elements in the network (e.g., Se, Kr, Sr). Because of this hindrance our calculations of the γ-process for $A \lesssim 90$, already very uncertain due to the effects of enhanced seed and temperature distributions, may require additional modification. For all heavier species, however, the γ-process should proceed unaffected by the background neutron flux that occurs in stellar zones concurrently experiencing explosive oxygen burning with peak temperatures $2.1 \lesssim T_9 \lesssim 3.2$.

This is obviously not so if the γ-process occurs in zones undergoing explosive carbon burning. Figure 4*a* shows that during the first 2×10^{-4} s of explosive carbon burning at $T_9 = 2.5$ a flux of roughly 3×10^{22} neutrons cm^{-3} is maintained. A flux of this magnitude is typical of *r*-process nucleosynthesis, but such an exposure time is far too short for the requisite beta-decays that typify the usual variety of *r*-process. As a result, seed nuclei may initially capture neutrons, but the flow eventually reaches a stagnation point caused by either strong reverse (γ, n) reactions or the depletion of neutrons (due in this case to the exhaustion of ^{22}Ne). For time $t \gtrsim 0.001$ s the free neutron abundance falls off rapidly and the heavy nuclei are driven back to the *proton*-rich side of the valley of beta-stability by (γ, n) reactions. Figure 4*a* shows that for explosive carbon burning at $T_9 = 2.5$, this reversal of flow from increasing neutron number to decreasing neutron number occurs at an elapsed time of about 0.01 s. At that time the temperature has dropped only 1%, but the neutron flux has decreased four orders of magnitude from its peak value. As a result, the γ-process can still proceed as previously described with only slight hindrance from a still rapidly decreasing neutron flux. A similar behavior is expected at higher temperatures.

At explosion temperatures lower than $T_{9m} \approx 2.5$, a somewhat altered behavior may occur in zones that experience carbon burning. The total neutron flux remains roughly constant but the peak value occurs over a longer exposure time. For temperatures $T_{9m} \lesssim 2.3$ the flux lasts so long that the "turn around" of flows described above does not occur until the temperature has fallen significantly. The remaining photon flux may not be sufficient to drive the γ-process, and a different sort of nucleosynthesis results that produces neutron-rich isotopes (Howard *et al.* 1972). Thus for explosive carbon burning at $T_{9m} \lesssim 2.3$ our present calculations may not be valid.

An intriguing possibility is the existence of stellar zones in close proximity, some of which experience a type of r-process and produce neutron-rich isotopes, and others which undergo the γ-process and produce p-nuclei. A mixture of such contiguous zones would be enhanced in both the r- and p- isotopes of xenon, for example. This is interesting because isotopic anomalies of this nature have been discovered in meteorites (cf. Reynolds and Turner 1964; Lewis, Srinivasan, and Anders 1975; Manuel, Hennecke, and Sabu 1972). Incorporation of relatively unmixed material from such zones into the early solar nebula either in the form of dust (Clayton 1975) or gas (Cameron and Truran 1977) might be a possible explanation.

Similar arguments to those given for neutrons pertain to the *proton* flux during explosive carbon and oxygen burning. Figure 4*b* shows the proton flux that results from the same explosive expansions discussed previously. Again, for oxygen burning, no modification of the γ-process is indicated. At $T_{9m} = 3.0$, for example, the proton abundance is at maximum 10^{-10} by mass fraction. At a density of 5×10^5 g cm^{-3} this implies a lifetime for ^{56}Fe against proton capture of about 10 s (Woosley *et al.* 1975). Heavier species will have still longer lifetimes against proton capture. Thus such reactions should be negligible within the context of a 1 second expansion time scale.

The proton flux from explosive carbon burning is much larger, a difference which once more is directly attributable to the greater efficiency of the $^{12}C + {}^{12}C$ reaction as opposed to $^{16}O + {}^{16}O$. For a peak temperature of either $T_{9m} = 2.5$ or 3.0 and a peak density of 5×10^5 g cm^{-3} the proton abundance is about 10^{-7} by mass fraction at an elapsed time of 0.01 s. Furthermore, the product of proton abundances and time scale remains roughly constant ($\sim 10^{-9}$ g s cm^{-3}) as the freeze-out proceeds at time $t > 0.01$ s. Under these conditions proton capture might be expected to occur on nuclei as heavy as $Z \approx 40$. In actuality not all nuclei of charge $Z < 40$ will be affected, for not only must the proton-induced reaction occur within the given time scale, but it must also compete with the (usually much stronger) photodisintegration flow. The criterion for modified behavior is then

$$\rho X_p \lambda_{p\gamma}(A, Z) \gtrsim \Lambda(A, Z)\,, \qquad (11)$$

where $\Lambda(A, Z)$ is the total photodisintegration rate of the nucleus (Z, A). This condition turns out to be satisfied only for the very lightest seed nuclei in the network which synthesize p-nuclei having $A \lesssim 100$. The synthesis of these light p-nuclei during explosive carbon burning may proceed in a much more complicated fashion than we have described, but given our present uncertain knowledge of the initial seed abundances and thermodynamics of the γ-process, we do not feel that a more complicated calculation is presently warranted.

To summarize, the γ-process is not greatly affected by the presence of free particle fluxes characteristic of explosive oxygen burning at $T_9 \approx 2.0$–3.0 (at least for nuclei having $A \gtrsim 90$), and if such zones are the site of the γ-process the present "perturbation" approach is justified. The γ-process *is* likely to be modified by the free particle fluxes present during explosive carbon burning at these temperatures, but may still function, although in a more complex manner. This suggests that the most promising, although not necessarily unique, astrophysical site for the process we have described is those stellar zones that, prior to explosion in a supernova, completed hydrostatic carbon burning. Such a picture would be consistent with the results of Pardo, Couch, and Arnett (1974), who find that an undesirable nucleosynthesis of lighter elements, e.g., ^{30}Si, results if carbon combusts at temperatures in excess of about 2.2×10^9 K. No such overproductions occur for explosive oxygen burning at temperatures $T_{9m} \approx 2.0$–3.0. In fact the light-element composition is ejected virtually unmodified.

V. CONCLUSIONS AND COMMENTS ON COSMOCHRONOLOGY

Clearly, from the arguments and discussion presented, the p- (or γ-) process is one of the most complicated of all nucleosynthetic processes. A proper calculation, of which this paper must be considered merely the forerunner, must necessarily involve (i) the detailed tracking of the composition of the preexplosive star (explicitly including the abundances of *all* stable elements from carbon to lead); (ii) accurate nuclear reaction rates for ~ 1100 nuclei (of which perhaps 100 are quite important); (iii) a correct detailed hydrodynamical treatment of the supernova explosion itself; and (iv) a network evolution of the abundances of elements at least up to $A \approx 110$ that includes the possibility of (p, γ), (p, n) (n, γ), (n, p), etc. reactions induced by the free neutron and proton baths librated during explosive carbon and/or oxygen burning as well as the photodisintegration chain downward from lead. Within the next few years such a proper calculation may actually become feasible. For now, though, we are content to point out some lessons to be learned from the present (relatively simple) investigation.

1. The solar abundances of the proton-rich nuclei suggest an origin for these species based upon the photodisintegration of heavier seed nuclei in which (γ, n), (γ, p), and (γ, α) reactions all play important roles. A continuum of temperatures in the range 2–3×10^9 K is required for time scales of roughly 1 second (although similar results are obtained with slightly lower temperatures and longer time scales). A likely site for the production of these species are those zones of supernovae that experience carbon and oxygen burning.

2. The preexplosive evolution of the composition of seed nuclei is an essential consideration for any calculation of p-nucleosynthesis.

3. The hydrogen-rich zones of novae and supernovae appear unlikely candidates for the sites of the bulk of p-nucleosynthesis. Calculations of the p-process in hydrogen-rich zones should not ignore the role played by weak interactions.

4. Isotopic anomalies in Xe found in meteorites might originate from the mixing of zones in supernovae that have undergone explosive carbon burning at slightly differing values of peak temperature or from material near the boundary of explosive carbon and oxygen burning.

5. The miniscule amount of ^{146}Sm produced by the γ-process implies that this species will not make a useful cosmochronometer. The species ^{92}Nb may be made in supernovae but its present abundance depends critically upon an uncertain half-life.

The last contention regarding ^{146}Sm differs markedly from previous investigations of the p-process. Audouze and Schramm (1972), using an interpolative scheme based upon the abundances and nuclear properties of p-nuclei, reasoned that a production ratio of ^{146}Sm/^{144}Sm in the range 0.35 to 0.60 should result from the p-process. This result was essentially confirmed by the more accurate network calculations of AT who obtained $^{146}\text{Sm}/^{144}\text{Sm} \gtrsim 1$, and the prediction met with apparent success when Notsu *et al.* (1973) reported the discovery of ^{142}Nd/^{144}Nd anomalies in meteorites that correlated with the elemental ratio of Sm/Nd in the samples (^{142}Nd is the decay produce of ^{146}Sm; ^{144}Nd is unaffected by the decay). From these observations Notsu *et al.* inferred the existence of a late spike of nucleosynthesis since ^{146}Sm ($\tau_{1/2} = 7 \times 10^7$ yr) would of necessity be incorporated into the meteorite within several half-lives of its formation. More recently, however, Lugmair, Scheinin, and Marti (1975) have reexamined these same samples and found no variation of ^{142}Nd/^{144}Nd, from which they inferred that there was no late spike of nucleosynthesis. We feel that this latter set of measurements is correct, i.e., that only an unmeasurably small amount of ^{146}Sm was present when the meteorite under examination formed, but we differ in the interpretation of these results. In our picture ^{146}Sm was not incorporated in the meteorite *because there never was a detectable amount to begin with!* Thus the absence of ^{142}Nd anomalies says nothing about the existence or nonexistence of a late spike of nucleosynthesis. In Table 5 we find that the average production ratio for ^{146}Sm/^{144}Sm is about 2%. That this ratio is a small number for the γ-process follows in an obvious manner from the larger photodisintegration cross section for ^{146}Sm as compared to ^{144}Sm (which has a magic number of neutrons) and the fact that the photodisintegration flows partially bypass ^{146}Gd (a possible proton-rich progenitor).

Another p-nucleus which might be a possible cosmochronometer is ^{92}Nb. Abt *et al.* (1974) claim tentative detection of ^{92}Nb in niobium metal extracted from the Earth's crust, from which they deduce a current value for the ratio $^{92}\text{Nb}/^{93}\text{Nb} = 1.5 \times 10^{-12}$. With an estimated half-life for ^{92}Nb of 1.7×10^8 yr (uncertain to a factor of 2), this implies $^{92}\text{Nb}/^{93}\text{Nb} \approx 10^{-4}$ at the time the Earth formed (uncertain to a factor of $\sim 10^8$). Abt *et al.* attribute this small primordial abundance to the p-process. Certainly our present calculations show this to be possible to within experimental error! As is shown in Table 5, the average production ratio ^{92}Nb/^{93}Nb is about 10^{-3} so that, even allowing for decay between the last supernova and solar system formation, the γ-process could be the origin of ^{92}Nb. However, given the current complex situation for the synthesis of p-nuclei lighter than $A \approx 110$ and the very uncertain value for the ^{92}Nb half-life (and even the existence of ^{92}Nb in the Earth's crust at all!), we feel that it would be premature to base any cosmochronological arguments on this species.

The authors are pleased to acknowledge the support of many host institutions during the 5 year course of this investigation, including Rice University, Los Alamos Scientific Laboratory, The University of Illinois, Lawrence Livermore Laboratory,[1] The California Institute of Technology, The University of California at Santa Cruz, and The Aspen Center for Physics. These calculations were made possible through the generous allocations of computer time by the Los Alamos and Lawrence Livermore Laboratories. One of us (S. E. W.) received support from the National Science Foundation, grant number AST 76-10933.

[1] Work was performed under the auspices of the U.S. Energy Research and Development Administration under contract W-7405-ENG-48.

APPENDIX A

NUCLEAR REACTION RATES

The reaction rates employed in these calculations have been generated using the statistical theory of nuclear reactions as formulated by Michaud and Fowler (1970). Their prescription for photon transmission functions was adopted without change. However, slight modifications were made in the radii Michaud and Fowler adopted for the equivalent square wells in the particle channels. In particular, we have employed the effective radius parameters from a determination by Truran (1972)

$$\begin{aligned} R_1(\text{fm}) &= 1.35 A_I^{1/3} + 0.1 \quad \text{nucleons}\,, \\ &= 1.23 A_I^{1/3} + 2.3 \quad \alpha\text{-particles}\,, \end{aligned} \tag{A1}$$

where A_I is the atomic mass of the nucleus I. It was felt that this parametrization was more appropriate for the heavier mass nuclei under consideration here, the somewhat small values of Michaud and Fowler being more correctly suited to the lighter intermediate-mass nuclei ($20 \leq A \leq 70$) with which they were concerned.

TABLE 7

CALCULATED PHOTONUCLEAR REACTION RATES IN s^{-1} FOR SELECTED SPECIES AT T_9 = 2.5 AND 3.0

	$T_9 = 2.5$			$T_9 = 3.0$		
SPECIES	$\lambda_{\gamma n}$	$\lambda_{\gamma p}$	$\lambda_{\gamma\alpha}$	$\lambda_{\gamma n}$	$\lambda_{\gamma p}$	$\lambda_{\gamma\alpha}$
^{202}Pb	1.2 (3)	5.5 (−5)	1.8 (−3)	1.5 (6)	2.0 (−1)	7.1 (−1)
^{201}Pb	3.8 (4)	2.0 (−4)	3.4 (−3)	1.5 (7)	5.0 (−1)	1.0 (0)
^{200}Pb	2.4 (2)	1.0 (−3)	2.5 (−2)	4.0 (5)	2.1 (0)	6.2 (0)
^{199}Pb	1.4 (4)	2.4 (−3)	3.5 (−2)	6.6 (6)	4.0 (0)	7.1 (0)
^{198}Pb	3.5 (1)	1.3 (−2)	5.3 (−1)	7.6 (4)	1.8 (1)	7.9 (1)
^{196}Pb	3.0 (1)	2.0 (−1)	9.6 (0)	8.3 (4)	1.8 (2)	8.8 (2)
^{194}Pb	1.0 (1)	2.1 (−1)	1.6 (2)	3.5 (4)	1.3 (3)	9.2 (3)
^{192}Pb	3.6 (0)	2.0 (1)	1.8 (3)	1.4 (4)	8.3 (3)	7.5 (4)
^{190}Pb	1.0 (−1)	2.3 (2)	4.7 (4)	4.3 (3)	6.2 (4)	1.4 (6)
^{197}Tl	2.3 (2)	9.6 (−1)	1.4 (−2)	3.5 (5)	6.4 (2)	4.7 (0)
^{196}Tl	2.1 (4)	2.0 (0)	1.0 (−2)	1.1 (7)	9.4 (2)	2.9 (0)
^{195}Tl	7.9 (0)	2.7 (1)	3.6 (−1)	1.6 (4)	8.7 (3)	7.0 (1)
^{194}Tl	3.0 (4)	5.7 (2)	3.5 (0)	1.9 (7)	1.5 (5)	4.9 (2)
^{193}Tl	2.8 (1)	7.6 (2)	1.6 (1)	6.1 (4)	1.4 (5)	1.7 (3)
^{191}Tl	1.8 (2)	6.8 (3)	2.9 (2)	4.7 (4)	8.6 (5)	1.8 (4)
^{192}Hg	4.0 (1)	6.7 (−3)	4.8 (−1)	8.8 (4)	1.2 (1)	8.0 (1)
^{190}Hg	4.5 (1)	2.0 (−1)	1.3 (1)	1.1 (5)	2.1 (2)	1.2 (3)
^{188}Hg	2.6 (1)	2.7 (0)	5.1 (2)	6.9 (4)	1.8 (3)	2.5 (4)
^{186}Hg	9.6 (−1)	1.0 (1)	1.2 (3)	3.5 (3)	5.6 (3)	5.3 (4)
^{184}Hg	2.0 (0)	5.6 (2)	9.6 (3)	8.1 (3)	1.8 (5)	3.0 (5)
^{188}Pt	1.4 (2)	1.3 (−2)	2.1 (1)	2.2 (5)	2.2 (1)	2.0 (3)
^{186}Pt	3.4 (2)	2.7 (−1)	8.6 (1)	5.9 (5)	2.4 (2)	6.4 (3)
^{184}Pt	6.6 (1)	9.1 (−1)	2.8 (2)	1.6 (5)	6.8 (2)	1.7 (4)
^{182}Pt	3.7 (0)	8.1 (0)	1.3 (3)	1.1 (4)	4.2 (3)	5.8 (4)
^{182}Os	1.0 (3)	9.1 (−2)	2.1 (1)	1.5 (6)	1.2 (2)	2.2 (3)
^{180}Os	3.9 (1)	5.8 (−1)	8.9 (1)	7.7 (4)	5.8 (2)	7.1 (3)
^{178}Os	2.6 (1)	7.9 (0)	5.3 (2)	6.5 (4)	5.0 (3)	3.0 (4)
^{176}Os	1.0 (0)	1.5 (2)	1.8 (3)	3.6 (3)	6.3 (4)	8.2 (4)
^{174}Os	7.8 (−1)	9.6 (2)	8.8 (3)	3.5 (3)	3.0 (5)	3.1 (5)
^{178}W	7.8 (2)	3.1 (−3)	1.6 (0)	1.1 (6)	8.1 (0)	2.8 (2)
^{176}W	6.0 (1)	5.2 (−2)	1.8 (1)	1.1 (5)	8.4 (1)	2.1 (3)
^{174}W	1.0 (1)	8.5 (−1)	8.9 (1)	2.5 (4)	8.6 (2)	7.6 (3)
^{172}W	4.0 (0)	8.3 (0)	5.5 (2)	1.4 (4)	5.4 (3)	3.3 (4)
^{170}W	8.0 (−1)	6.4 (1)	1.1 (3)	3.6 (3)	3.0 (4)	5.7 (4)
^{180}Ta	9.5 (5)	1.4 (3)	6.9 (−2)	2.5 (8)	2.9 (0)	2.0 (1)
^{172}Hf	5.7 (1)	1.9 (−2)	3.0 (0)	1.1 (5)	3.8 (1)	4.9 (2)
^{170}Hf	3.4 (1)	1.3 (−1)	1.1 (1)	8.3 (4)	1.8 (2)	1.4 (3)
^{168}Hf	2.3 (0)	6.2 (−1)	2.1 (1)	9.0 (3)	6.7 (2)	2.4 (3)
^{166}Hf	3.3 (−1)	5.0 (0)	5.4 (1)	1.6 (3)	3.9 (3)	5.3 (3)
^{164}Hf	4.1 (−1)	2.9 (1)	2.9 (2)	2.0 (3)	1.7 (4)	2.1 (4)
^{168}Yb	2.1 (2)	5.0 (−4)	2.2 (−1)	3.7 (5)	1.5 (0)	6.0 (1)
^{166}Yb	3.0 (1)	2.7 (−3)	9.0 (−1)	7.3 (4)	6.0 (0)	2.0 (2)
^{164}Yb	3.0 (0)	3.2 (−2)	4.8 (0)	1.0 (4)	4.7 (1)	7.8 (2)
^{162}Yb	7.0 (−1)	1.2 (0)	5.5 (1)	3.0 (3)	1.2 (3)	5.8 (3)
^{160}Yb	3.0 (−1)	7.6 (0)	1.6 (3)	1.3 (3)	5.4 (3)	9.4 (4)
^{164}Er	4.6 (2)	2.7 (−4)	4.2 (−2)	6.9 (5)	1.2 (0)	1.6 (1)
^{162}Er	6.5 (1)	2.7 (−3)	2.0 (−1)	1.3 (5)	7.9 (0)	6.0 (1)
^{160}Er	8.8 (0)	4.5 (−2)	1.7 (0)	2.5 (4)	8.2 (1)	3.6 (2)
^{158}Er	2.0 (0)	3.9 (−1)	9.6 (1)	7.1 (3)	4.9 (2)	1.0 (4)
^{156}Er	8.0 (0)	5.6 (−1)	6.3 (3)	2.4 (4)	6.1 (2)	3.1 (5)
^{158}Dy	1.1 (2)	1.6 (−4)	2.0 (−2)	2.0 (5)	7.0 (−1)	9.3 (0)
^{156}Dy	2.1 (1)	8.7 (−4)	1.2 (0)	5.0 (4)	2.7 (0)	2.8 (2)
^{154}Dy	6.0 (1)	3.5 (−3)	2.6 (2)	1.3 (5)	8.9 (0)	2.4 (4)
^{152}Dy	1.0 (1)	5.0 (−2)	8.7 (3)	2.7 (4)	8.3 (1)	4.4 (5)
^{150}Dy	1.2 (1)	6.1 (−1)	1.5 (5)	3.5 (4)	5.8 (2)	4.7 (6)
^{154}Gd	5.0 (2)	1.6 (−5)	9.0 (−2)	6.5 (5)	1.2 (−1)	3.3 (1)
^{152}Gd	7.7 (2)	4.0 (−5)	3.3 (1)	9.7 (5)	2.5 (−1)	4.7 (3)
^{150}Gd	2.4 (2)	4.7 (−4)	4.8 (2)	3.4 (5)	1.7 (0)	4.3 (4)
^{148}Gd	5.4 (1)	1.8 (−2)	4.1 (3)	1.0 (5)	5.0 (1)	2.5 (5)
^{146}Gd	1.2 (−2)	9.1 (−1)	3.0 (−2)	9.6 (1)	1.0 (3)	1.4 (1)
^{145}Eu	1.8 (−2)	4.0 (2)	3.6 (−3)	8.7 (1)	8.5 (4)	2.4 (0)
^{148}Sm	2.1 (3)	2.3 (−5)	4.5 (1)	1.8 (6)	1.8 (−1)	6.0 (3)
^{146}Sm	4.5 (2)	1.2 (−4)	5.9 (2)	5.0 (5)	6.4 (−1)	5.3 (4)
^{144}Sm	1.9 (−2)	1.5 (−2)	2.0 (−3)	1.1 (2)	3.0 (1)	1.4 (0)
^{142}Sm	2.7 (−3)	1.0 (−1)	1.7 (−2)	2.3 (1)	1.6 (2)	8.6 (0)
^{140}Sm	2.0 (−3)	1.2 (1)	4.5 (−1)	1.1 (1)	1.0 (4)	1.4 (2)

TABLE 7—*Continued*

Species	$T_9 = 2.5$ $\lambda_{\gamma n}$	$\lambda_{\gamma p}$	$\lambda_{\gamma \alpha}$	$T_9 = 3.0$ $\lambda_{\gamma n}$	$\lambda_{\gamma p}$	$\lambda_{\gamma \alpha}$
^{144}Nd	4.3 (3)	5.6 (−6)	1.2 (2)	3.1 (6)	5.7 (−2)	1.4 (4)
^{142}Nd	7.3 (−1)	9.0 (−5)	3.7 (−4)	2.2 (3)	2.9 (−1)	3.3 (−1)
^{140}Nd	2.4 (−1)	4.2 (−3)	8.0 (−3)	1.0 (3)	1.0 (1)	5.1 (0)
^{138}Nd	1.5 (−1)	2.6 (−1)	1.6 (−1)	8.0 (2)	3.7 (2)	6.6 (1)
^{136}Nd	5.6 (−3)	3.6 (0)	5.6 (−1)	3.0 (1)	3.7 (3)	1.8 (2)
^{138}Ce	3.8 (0)	9.3 (−5)	5.8 (−4)	9.3 (3)	5.2 (−1)	5.6 (−1)
^{136}Ce	2.8 (0)	2.2 (−3)	8.2 (−3)	9.5 (3)	6.6 (0)	5.8 (0)
^{134}Ce	1.1 (−1)	3.5 (−2)	1.0 (−1)	5.1 (2)	7.3 (1)	4.8 (1)
^{132}Ce	5.8 (−2)	1.2 (−1)	5.0 (−1)	4.0 (2)	1.7 (2)	1.8 (2)
^{130}Ce	9.8 (−3)	2.5 (0)	2.3 (0)	4.6 (1)	2.1 (3)	6.3 (2)
^{138}La	6.5 (3)	2.5 (−3)	3.0 (−6)	2.8 (6)	5.1 (0)	8.4 (−3)
^{132}Ba	1.2 (0)	1.1 (−4)	2.2 (−3)	3.6 (3)	5.8 (−1)	2.0 (0)
^{130}Ba	9.3 (−1)	1.0 (−3)	1.7 (−2)	3.7 (3)	3.1 (0)	1.1 (1)
^{128}Ba	2.1 (−1)	2.7 (−2)	7.5 (−2)	1.1 (3)	5.0 (1)	3.9 (1)
^{126}Ba	4.8 (−2)	7.7 (−1)	7.0 (−1)	3.1 (2)	8.3 (2)	2.5 (2)
^{124}Ba	8.8 (−5)	1.9 (1)	1.6 (1)	6.6 (−1)	1.2 (4)	3.4 (3)
^{126}Xe	3.4 (−1)	3.4 (−4)	2.3 (−3)	1.2 (3)	1.5 (0)	2.3 (0)
^{124}Xe	5.2 (−1)	1.4 (−2)	9.6 (−2)	2.1 (3)	3.2 (1)	5.1 (1)
^{122}Xe	7.4 (−2)	3.2 (−1)	1.7 (0)	4.2 (2)	4.9 (2)	5.8 (2)
^{120}Xe	7.4 (−3)	2.3 (1)	1.4 (2)	5.2 (1)	1.7 (4)	2.2 (4)
^{122}Te	7.2 (−1)	5.7 (−5)	2.6 (−2)	2.1 (3)	3.6 (−1)	1.8 (1)
^{120}Te	9.9 (−2)	3.6 (−3)	8.8 (−1)	4.2 (2)	1.1 (1)	3.6 (2)
^{118}Te	2.7 (−2)	2.6 (−1)	3.2 (1)	1.4 (2)	4.2 (2)	7.2 (3)
^{116}Te	3.1 (−3)	3.1 (0)	1.0 (2)	2.4 (1)	3.4 (3)	1.9 (4)
^{115}Sn	4.7 (2)	4.8 (−7)	9.8 (−7)	2.5 (5)	6.3 (−3)	4.1 (−3)
^{114}Sn	1.8 (−2)	2.3 (−5)	5.7 (−5)	7.7 (1)	1.9 (−1)	1.0 (−1)
^{112}Sn	9.6 (−3)	2.2 (−3)	2.6 (−3)	6.0 (1)	7.4 (0)	2.8 (0)
^{110}Sn	2.0 (−3)	1.8 (−1)	6.4 (−2)	1.7 (1)	3.2 (2)	4.1 (1)
^{108}Sn	9.8 (−5)	6.1 (0)	1.5 (0)	1.4 (0)	5.7 (3)	5.4 (2)
^{108}Cd	1.0 (−1)	1.9 (−5)	1.4 (−3)	4.4 (2)	9.3 (−2)	1.7 (0)
^{106}Cd	9.9 (−3)	2.0 (−3)	2.6 (−2)	6.7 (1)	5.8 (0)	2.1 (1)
^{104}Cd	3.6 (−4)	3.7 (−1)	1.4 (−1)	4.5 (0)	6.2 (2)	8.6 (1)
^{102}Cd	*	1.5 (1)	3.6 (0)	*	1.3 (4)	1.2 (3)
^{104}Pd	2.9 (−1)	1.2 (−6)	1.1 (−3)	9.9 (2)	1.2 (−2)	1.4 (0)
^{102}Pd	3.1 (−2)	2.9 (−4)	1.1 (−2)	1.6 (2)	1.0 (0)	1.1 (1)
^{100}Pd	4.0 (−3)	2.8 (−2)	1.5 (−1)	3.0 (1)	5.8 (1)	1.0 (2)
^{98}Pd	*	5.2 (0)	6.0 (−1)	*	5.7 (3)	3.0 (2)
^{100}Ru	8.5 (−1)	1.8 (−6)	1.5 (−3)	2.2 (3)	2.4 (−2)	1.6 (0)
^{98}Ru	7.3 (−2)	1.7 (−4)	2.9 (−2)	2.9 (2)	8.9 (−1)	2.5 (1)
^{96}Ru	8.8 (−3)	3.1 (−2)	3.4 (−1)	5.0 (1)	8.0 (1)	2.1 (2)
^{94}Ru	*	4.7 (0)	8.6 (−8)	*	5.1 (3)	5.7 (−4)
^{96}Mo	2.7 (0)	9.8 (−7)	8.9 (−3)	4.7 (3)	1.4 (−2)	7.0 (0)
^{94}Mo	3.2 (−1)	4.9 (−5)	2.8 (−1)	8.3 (2)	3.0 (−1)	1.7 (2)
^{92}Mo	1.4 (−6)	2.8 (−2)	1.0 (−8)	3.7 (−2)	7.0 (1)	9.8 (−5)
^{90}Mo	8.0 (−8)	1.8 (0)	5.9 (−7)	3.3 (−3)	1.9 (3)	2.6 (−3)
^{93}Nb	5.9 (0)	4.0 (−1)	2.3 (−1)	7.9 (3)	3.5 (2)	1.3 (2)
^{92}Nb	1.4 (2)	1.2 (0)	2.2 (−7)	9.4 (4)	6.7 (2)	1.4 (−3)
^{94}Zr	4.9 (1)	2.1 (−9)	3.4 (−5)	4.1 (4)	6.8 (−5)	4.2 (−2)
^{92}Zr	9.7 (0)	5.7 (−8)	1.0 (−2)	1.1 (4)	9.2 (−4)	6.4 (0)
^{90}Zr	1.8 (−5)	1.9 (−4)	1.6 (−10)	2.8 (−1)	8.8 (−1)	2.4 (−6)
^{88}Zr	7.6 (−6)	1.2 (−3)	1.2 (−7)	1.4 (−1)	4.1 (0)	6.5 (−4)
^{88}Sr	3.4 (−4)	3.0 (−9)	1.3 (−12)	2.7 (0)	8.2 (−5)	5.9 (−8)
^{86}Sr	3.0 (−4)	1.4 (−6)	8.6 (−9)	3.1 (0)	1.4 (−2)	9.0 (−5)
^{84}Sr	1.2 (−5)	7.1 (−5)	3.1 (−6)	1.9 (−1)	5.3 (−1)	1.5 (−2)
^{82}Sr	4.1 (−5)	4.4 (−2)	1.1 (−3)	6.5 (−1)	9.7 (1)	1.9 (0)
^{84}Kr	1.4 (−2)	6.4 (−9)	4.9 (−10)	6.8 (1)	1.9 (−4)	9.6 (−6)
^{82}Kr	2.1 (−3)	1.7 (−7)	2.1 (−7)	1.5 (1)	2.4 (−3)	1.3 (−3)
^{80}Kr	8.4 (−5)	3.9 (−5)	2.4 (−5)	9.2 (−1)	2.7 (−1)	8.8 (−2)
^{78}Kr	3.8 (−5)	3.1 (−3)	6.0 (−4)	5.7 (−1)	1.8 (1)	1.4 (0)
^{80}Se	1.3 (−1)	3.1 (−10)	2.7 (−9)	3.9 (2)	1.6 (−5)	4.1 (−5)
^{78}Se	4.2 (−3)	2.5 (−8)	4.7 (−7)	2.1 (1)	6.0 (−4)	2.4 (−3)
^{77}Se	4.6 (2)	1.1 (−6)	1.8 (−5)	2.1 (5)	1.4 (−2)	1.1 (−1)
^{76}Se	7.7 (−4)	2.5 (−6)	9.6 (−5)	6.2 (0)	1.8 (−2)	2.8 (−1)
^{74}Se	2.8 (−5)	1.0 (−3)	1.1 (−2)	4.5 (−1)	4.5 (0)	1.7 (1)

* Reaction link not in network.

Using the above parametrization, we calculated thermonuclear reaction rates for more than 1000 nuclei. Most of the binding energies employed have experimental determinations (Wapstra and Gove 1971). We emphasize this point because the particle separation energies play such a key role in the γ-process. For those few nuclei on the proton-rich side of the valley of beta-stability that we chose to include but for which experimental mass determinations were not available, the mass relations of Garvey *et al.* (1969) were employed. Ground-state spin and parity information and excitation energies of the first excited state (used in computing photon widths) were taken, when available, from Lederer, Hollander, and Perlman (1967). For nuclei with unknown spin and parity a Nilsson level diagram (Seeger and Howard 1975) was employed. Using this information the thermally averaged rate factor,

$$\lambda_{ij} = N_A\langle\sigma_{ij}v\rangle = \frac{3.73 \times 10^{10}}{\hat{A}_i^{1/2}T_9^{3/2}} \int_0^\infty \bar{\sigma}_{ij}E_i \exp(-11.605E_i/T_9)dE_i \text{ cm}^3 \text{ mole}^{-1} \text{ s}^{-1}\,, \tag{A2}$$

for the six reactions (n, γ), (p, γ), (p, n), (α, p), (α, γ), and (α, n) were computed. In the above formula $\bar{\sigma}_{ij}$ is the average cross section in barns for the reaction $I(i, j)J$ at center of mass energy E_i in MeV and $\hat{A}_i$ is the reduced mass of the reactants in the entrance channel. In addition, rate factors were computed for the inverses of each of the six varieties of reactions using the principle of reciprocity (cf. Fowler, Caughlan, and Zimmerman 1967). In particular the photodisintegration rates, which are the only pertinent ones for the present treatment, are given by

$$\lambda_{\gamma i} = 9.87 \times 10^9\left(\frac{g_I g_i}{g_J}\right)\left(\frac{A_I A_i}{A_J}\right)^{3/2}\lambda_{i\gamma} \exp(-11.605S_i/T_9) \text{ cm}^3 \text{ mole}^{-1} \text{ s}^{-1}\,, \tag{A3}$$

where g_I is the ground state partition function for the nucleus I in the reaction $I(i, j)J$, A_I is its atomic mass, $\lambda_{i\gamma}$ is given by equation (A2), and S_i is the separation energy of the particle i in MeV.

Approximately 300 of the photodisintegration reactions considered most important to the present work are given in Table 7. For the most part entries have not been given for odd nuclei and odd-mass nuclei, even though they were of course included in all calculations. The destruction of such nuclei is always dominated by large (γ, n) rates and are therefore uninteresting as branching points or waiting points. Typically the photoneutron rate for an odd nucleus at the temperatures we are considering ($2 \leq T_9 \leq 3$) is about 100 times more rapid than for neighboring even nuclei.

The effects of nuclear excited states have not been included in our calculations because of the large amount of computer time that would be required for their proper treatment. Except for the photon channel, it was assumed that a given compound nuclear state could decay only to the ground state of a given particle channel. Though this assumption has been customary in past astrophysical calculations like those of Michaud and Fowler (1970) and Truran (1972), recent studies of Woosley *et al.* (1975) have shown that such neglect can lead to sizable errors. In particular, a (p, γ) cross-section calculation that neglects the presence of a high density of outgoing states in the neutron channel will yield a gross overestimate of the actual cross section. This is particularly true if the Gamow peak energy, $E_0 = 0.122(Z_1^2Z_2^2\hat{A}T_9^2)^{1/3}$ MeV, exceeds the threshold for the (p, n) reaction. Similar considerations hold for the alpha channel where excited states in both the proton and neutron channel may compete with the gamma channel. Because we deal here exclusively with nuclei that are proton-rich, these problems are not so severe as they might be for a nucleus closer to the center of the valley of the beta stability. Reactions with neutrons in an outgoing channel are characterized here by highly endoergic Q-values. Thus the full effect of the neutron channel competition is not felt until the temperature becomes fairly high. However, the competition of compound nuclear inelastic proton scattering with (p, γ) will be important, as will the competition of (α, p) with (α, γ) reactions to various excited states of the proton channel. As a result, the numbers we calculate here for the radiative capture of charged particles (and thus for photodisintegration rates) are probably overestimates of the actual values. We estimate that for the proton-rich nuclei with which we are especially concerned these errors will amount to as much as a factor of 3 to 10 for (p, γ) reactions and factors of 5 to 50 for (α, γ) reactions. The largest errors will occur for the highest temperatures considered here, namely $T_9 \approx 3$. So long as the errors are systematic and do not vary greatly from nucleus to nucleus, the nucleosynthesis we have calculated should not be grossly affected, although we do note that a sizable decrease in (γ, α) rates relative to (γ, p) rates might result in large amounts of material flowing through nuclei with odd values of Z.

Detailed printouts of all rates employed in these calculations are available from the authors upon request.

APPENDIX B

SOLUTION OF A PHOTODISINTEGRATION NETWORK

Consider a group of differential equations for the form

$$\frac{dY_k}{dt} = -Y_k\Lambda_k + Y_{k+n}\lambda_{\gamma n}(k + n) + Y_{k+p}\lambda_{\gamma p}(k + p) + Y_{k+\alpha}\lambda_{\gamma\alpha}(k + \alpha)\,, \tag{B1}$$

where we have employed the definition $Y_k = X_k/A_k$, i.e., the mass fraction of the species k divided by its atomic mass number (integer), and $\Lambda_k \equiv \lambda_{\gamma n}(k) + \lambda_{\gamma p}(k) + \lambda_{\gamma \alpha}(k)$ is its total photodisintegration rate. The notation "$k + n$," "$k + p$," and "$k + \alpha$" refer to those species that can decay to the nucleus k by ejection of a neutron, proton, or α-particle, respectively (if such nuclei are included in the network). This group of equations can be easily linearized and evolved numerically *without the necessity of matrix inversion*. Simply order the equations in terms of decreasing nuclear charge and atomic weight, i.e., $(Z_{\max}, A_{\max})$, $(Z_{\max}, A_{\max} - 1)$, $\ldots$, $(Z_{\max} - 1, A_{\max})$ etc., where $A_{\max}$ is the isotope with highest mass of given nuclear charge. Then the linearized equation for species number 1 is

$$Y_1^{(j+1)} = Y_1^{(j)}/(1 + \Lambda_1^{(j+1)}\Delta t)\,, \qquad \Delta t = t^{(j+1)} - t^{(j)}\,, \tag{B2}$$

where the superscripts indicate the time step of the evaluation, e.g., $t^{(j+1)}$ is the elapsed time after $j + 1$ steps. The abundance of the kth species at the time $t^{(j+1)}$ is given by the recursion relation

$$\begin{aligned} Y_k^{(j+1)} = \{[&Y_{k+n}^{(j+1)}\lambda_{\gamma n}^{(j+1)}(k + n) + Y_{k+p}^{(j+1)}\lambda_{\gamma p}^{(j+1)}(k + p) + Y_{k+\alpha}^{(j+1)}\lambda_{\gamma \alpha}^{(j+1)}(k + \alpha)]\Delta t \\ &+ Y_k^{(j)}\}(1 + \Lambda_k^{(j+1)}\Delta t)^{-1}\,. \end{aligned} \tag{B3}$$

This system of equations can be evolved numerically on any medium-sized computer. As an economy measure reaction rates can be updated only when the temperature has changed significantly. We employed the criterion $\Delta T_9/T_0 > 1\%$. Time steps were chosen so that no species of interest changes its abundance by more than 15% in any given interval.

REFERENCES

Abt, K. E., Knight, J. D., Camp, D. C., and Perkins, R. W. 1974, *Geochim. Cosmochim. Acta*, **38**, 4185.
Agnese, A., La Camera, M., and Wataghin, A. 1969, *M.N.R.A.S.*, **146**, 58.
Amiet, J. P., and Zeh, H. D., 1967, *Phys. Letters*, **2513**, 305.
———. 1968, *Zeit. f. Physik*, **217**, 485.
Arnett, W. D. 1969, *Ap. J.*, **157**, 1369.
Arnett, W. D., and Truran, J. W. 1969, *Ap. J.*, **157**, 339.
Arnould, M. 1976, *Astr. Ap.*, **46**, 117.
Arnould, M., and Brihaye, C. 1969, *Astr. Ap.*, **1**, 193.
Audouze, J. 1970, *Astr. Ap.*, **8**, 436.
Audouze, J., and Schramm, D. N. 1972, *Nature*, **237**, 447.
Audouze, J., and Truran, J. W. 1975, *Ap. J.*, **202**, 204 (AT).
Burbidge, E. M., Burbidge, G. R., Fowler, W. A., and Hoyle, F. 1957, *Rev. Mod. Phys.*, **29**, 547 (B^2FH).
Cameron, A. G. W. 1957, *Chalk River Rept.* CRL-41; see also 1957, *Pub. A.S.P.*, **69**, 201.
———. 1959, *Ap. J.*, **130**, 452.
———. 1973, *Space Sci. Rev.*, **15**, 121.
Cameron, A. G. W., and Truran, J. W. 1977, *Icarus*, **30**, 447.
Clayton, D. D. 1975, *Ap. J.*, **199**, 765.
———. 1976, *Geochim. Cosmochim. Acta*, **40**, 563.
Couch, R. G., Schmiedekamp, A. B., and Arnett, W. D. 1974, *Ap. J.*, **190**, 95.
Fowler, W. A., Caughlan, G., and Zimmerman, B. A. 1967, *Ann. Rev. Astr. Ap.*, **5**, 525.
Frank-Kamenetskii, D. A. 1961, *Soviet Astr.*, **5**, 66.
Garvey, G. T., Gerace, W. J., Jaffe, R. L., Talmi, I., and Kelson, I. 1969, *Rev. Mod. Phys.*, **41**, 51.
Hainebach, K. L., Schramm, D. N., and Blake, J. B. 1976, *Ap. J.*, **205**, 920.
Howard, W. M., Arnett, W. D., Clayton, D. D., and Woosley, S. E. 1972, *Ap. J.*, **172**, 201.
Ito, K. 1961, *Progr. Theoret. Phys.*, **26**, 990.
Joukoff, A. A. 1969, *Astr. Ap.*, **3**, 186.
Lamb, S. A., Howard, W. M., Truran, J. W., and Iben, I., Jr. 1977, *Ap. J.*, **217**, 213.
Lamb, S. A., Iben, I., Jr., and Howard, W. M. 1976, *Ap. J.*, **207**, 209.
Lederer, C. M., Hollander, J. M., and Perlman, I. 1967, *Table of Isotopes* (6th ed.; New York: Wiley).
Lewis, R. S., Srinivasan, B., and Anders, E. 1975, *Science*, **190**, 1251.
Lugmair, G. W., Scheinin, N. B., and Marti, K. 1975, *Earth Planet. Sci. Letters*, **27**, 79.
Macklin, R. L. 1970, *Ap. J.*, **162**, 353.
Malkiel, G. S. 1963, *Soviet Astr.*, **7**, 207.
Manuel, O. K., Hennecke, E. W., and Sabu, D. D. 1972, *Nature*, **240**, 99.
Michaud, G., and Fowler, W. A. 1970, *Phys. Rev. C*, **2**, 2041.
———. 1972, *Ap. J.*, **173**, 157.
Notsu, K., Nabuchi, H., Yoshioka, O., Matsuda, K. and Ozima, M. 1973, *Earth Planet. Sci. Letters*, **19**, 29.
Pardo, R. C., Couch, R. G., and Arnett, W. D. 1974, *Ap. J.*, **191**, 711.
Reeves, H., and Stewart, P. 1965, *Ap. J.*, **141**, 1432.
Reynolds, J. H., and Turner, G. 1964, *J. Geophys. Res.*, **69**, 3263.
Schramm, D. N., and Arnett, W. D. 1975, *Ap. J.*, **198**, 629.
Seeger, P. A., and Howard, W. M. 1975, *Nucl. Phys.*, **A238**, 491.
Starrfield, S., Truran, J. W., and Sparks, W. M. 1975, *Ap. J. (Letters)*, **198**, L113.
Takahashi, K., Yamada, M., and Kondoh, T. 1973, *Atomic Data and Nuclear Data Tables*, **12**, 101.
Truran, J. W. 1972, *Ap. Space Sci.*, **18**, 308.
———. 1973, in *Explosive Nucleosynthesis*, ed. D. N. Schramm, and W. D. Arnett (Austin: University of Texas Press).
Truran, J. W., and Arnett, W. D. 1970, *Ap. J.*, **160**, 181.
Truran, J. W., and Cameron, A. G. W. 1972, *Ap. J.*, **171**, 89.
Wapstra, A. H., and Gove, N. D. 1971, *Nucl. Data Tables*, **9**, 265.
Woosley, S. E., Arnett, W. D., and Clayton, D. D. 1973, *Ap. J. Suppl.*, **26**, 231 (WAC).
Woosley, S. E., Fowler, W. A., Holmes, J. A., and Zimmerman, B. A. 1975, Caltech Orange Aid Preprint OAP-422.

W. M. HOWARD: T-Division, L-71, University of California, Lawrence Livermore Laboratory, Livermore, CA 94550

S. E. WOOSLEY: Lick Observatory, Board of Studies in Astronomy and Astrophysics, University of California, Santa Cruz, CA 95064